Accelerated Cosmic Expansion as Evidence for Black Hole Cosmology

Hyoyoung Choi[1*]

1 Independent Researcher, Gunsan, Republic of Korea.

$*$ E-mail:7icarus7@gmail.com

Abstract

Black Hole Cosmology has traditionally been challenged by the apparent incompatibility between black hole interiors and cosmic expansion. However, because classical general relativity, on which this criticism is based, is itself incomplete in black hole interiors, the criticism rests on an incomplete premise. We reformulate this problem using total gravitational self-energy (GSE). The total GSE functional $U_{gs-T}(R) = -\frac{\beta G M_{fr}^2}{R}\left(1 - \frac{5\beta}{7}\frac{G M_{fr}}{c^2 R}\right)$ contains a negative GSE term and a positive matter–GSE interaction term responsible for the repulsive radial response, where β denotes the structural coefficient of the GSE functional. For a matter-filled black hole interior, this energy landscape yields finite radii, including $R_{gs} = (5\beta/7)R_S$, $R_{\min,BH} = 5\beta R_S/(14 - 5\beta)$, and $R_{\min,E} = (5\beta/14)R_S$. Thus, the point singularity is replaced by a finite-radius structure, allowing sufficiently massive black holes to contain macroscopic nonsingular interiors. This supports the possibility of closed black hole universes whose interiors exhibit weak local curvature and small tidal gradients. For our observable universe, the relevant configuration is not an isolated vacuum black hole, but a cosmological black hole embedded in a much larger, nearly homogeneous matter distribution. The matter-sector mass enclosed within the present particle horizon gives a Schwarzschild-equivalent event horizon radius $R_S \simeq 150.4$ Gly, whereas the causal radius is $R_U \simeq 46.5$ Gly, giving $R_S/R_U \simeq 3.23 > 1$. In this compactness sense, the observable universe lies within its own Schwarzschild-equivalent radius. The cosmological application of total GSE yields the dark energy density $\rho_{\Lambda_m} = \frac{\beta \rho_m}{2}\frac{R_S}{R_U}\left(\frac{5\beta}{14}\frac{R_S}{R_U} - 1\right)$. Under the matter-dominated background approximation with $w_{\Lambda_m} \simeq -1$, the condition for accelerated expansion is $\rho_{\Lambda_m} > \rho_m/2$, or equivalently, $R_U < R_{\mathrm{crit,U}} \simeq 0.279\,\beta R_S$. The framework provides a three-stage interpretation of cosmic history: early accelerated expansion driven by total GSE, a decelerating phase during the radiation era and the matter era, and late-time accelerated expansion driven by total GSE dark energy. Thus, accelerated cosmic expansion is not evidence against Black Hole Cosmology, but rather a central signature of a cosmological black hole. The predicted dark energy density provides a direct observational test of this interpretation of the observable universe.

Contents

1 Introduction

1.1 Historical Background of Black Hole Cosmology

The possibility that the universe itself may exist inside a black hole interior has appeared in several forms since the 1970s. One of the earliest explicit examples is Pathria's proposal that the universe may be compared with a black hole by relating its cosmological mass and radius to the corresponding Schwarzschild radius [1]. The basic motivation comes from comparing a cosmological mass and radius scale with the Schwarzschild radius,

$$R_S = \frac{2GM}{c^2}. \tag{1}$$

If a mass M is enclosed within a sufficiently large radius R, the associated Schwarzschild radius can become comparable to, or even larger than, the physical radius of the system. This observation gave rise to the historical "universe as a black hole" argument.

A related line of thought appeared in the idea of nested or "Chinese" universes, in which black hole interiors may be connected to other cosmic domains [2]. Later developments considered the possibility that black holes formed through astrophysical collapse could contain internal universes, baby universes, or a black hole multiverse [3,4]. In this broader class of scenarios, each sufficiently massive black hole may form its own internal cosmological domain. Black hole formation can then be viewed as a possible channel through which new universe type regions arise.

The present paper belongs to this broad historical family of Black Hole Cosmology (BHC), but it introduces a different dynamical mechanism. Instead of relying only on the classical Schwarzschild interior picture, we analyze the interior of a self gravitating configuration using total gravitational self-energy (GSE) dynamics. This work also extends earlier GSE based approaches to the problems of Black Hole Cosmology [5] by using the two term total GSE structure developed in the later total GSE framework [6,7]. Within this framework, the singularity problem, the apparent absence of habitable interior regions, and the expansion problem can be reconsidered in terms of total GSE dynamics.

1.2 Standard Objections to Black Hole Cosmology

Despite its historical interest, BHC has not become a mainstream cosmological model because it appears to face several serious conceptual problems. These problems are not usually presented as a single formal no-go theorem. Rather, they arise from comparing the classical black hole interior picture with the observed properties of our universe. They were also summarized in an earlier discussion of the problems of Black Hole Cosmology [5]. The main objections can be stated as follows.

1) **The singularity problem.**

   A classical Schwarzschild black hole interior contains a singular future boundary. In the classical collapse picture, infalling matter is driven toward a singular limit rather than toward a large, stable, matter filled region [8–11]. Therefore, the conventional black hole interior picture does not provide a satisfactory explanation for how galaxies, stars, planetary systems, and observers could exist inside a black hole universe.

2) **The time-direction problem.**

   The location of the singular point along the time direction appears to differ between the usual black hole interior description and standard cosmology. In the usual black hole interior description, the singular point lies in the future of infalling matter. By contrast, in cosmological discussions, the Big Bang singularity lies in the past [8, 12]. In the conventional interpretation, the future singular point of a black hole and the past Big Bang singularity of cosmology do not coincide.

3) **The expansion problem.**

   Cosmic expansion appears to contradict the black hole interpretation. The standard intuition associates a black hole interior with inward evolution and collapse. The observed universe, however, expands, and observations of Type Ia supernovae, the cosmic microwave background, and baryon acoustic oscillations support a late time accelerated expansion [13–16]. For this reason, cosmic expansion has often been regarded as one of the strongest objections to BHC.

Taken at face value, these objections have made BHC appear physically untenable and have prevented it from becoming a mainstream cosmological model.

1.3 Conceptual Limitations of the Standard Objections

The objections summarized above are serious for a naive vacuum Schwarzschild interpretation of black hole interiors. However, they do not by themselves constitute a final disproof of Black Hole Cosmology. They rely on extrapolating the unmodified classical description into regimes where that description is already known, or strongly suspected, to be incomplete [8, 10, 11]. The main conceptual limitations can be summarized as follows.

1) **The black hole interior is not experimentally fixed.**

   There is no observationally confirmed consensus model for the physical interior metric of a black hole. General relativity has been extensively tested outside black holes, but it has not been directly tested inside black holes. Since the classical theory predicts a singular limit in black hole interiors [8, 11], this prediction itself signals the need for a completion or modification in that regime. Wald explicitly describes the prediction of singularities as a "breakdown of general relativity", because the classical description cannot be expected to remain valid near a spacetime singularity [17, p. 212]. Therefore, arguments based only on the unmodified classical interior solution are not sufficient to give final conclusions about the physical endpoint of collapse or about the possible internal structure of a black hole universe.

2) **Classical general relativity faces completion problems in extreme regimes.**

   Modern gravitational physics commonly treats these unresolved phenomena through separate supplementary sectors or mechanisms. Their possible interpretation as manifestations of a common incompleteness in the physical implementation of the gravitational source is developed in detail in Ref. [7]. The conventional associations are summarized in Table 1.

   Each of these approaches provides a possible description of an individual phenomenon and is supported by its own observational or theoretical literature. However, their existence does not establish that classical General Relativity is already complete throughout finite black hole interiors and at macroscopic cosmological scales. As argued more fully in Ref. [7], the continued need for several independent supplementary sectors leaves open the possibility that some of these apparently separate problems reflect a common incompleteness in the physical implementation of the gravitational source.

Unresolved problem	**Supplementary sector or mechanism**
Primordial accelerated expansion	An inflaton field [18–20]
Gravitational phenomena of galaxies and galaxy clusters	Nonbaryonic dark matter [15, 21, 22]
Late-time cosmic accelerated expansion	A cosmological constant or an independent dark energy sector [13, 14, 16, 23]
Black hole singularities	An unknown quantum-gravitational or nonsingular-interior mechanism [11, 24, 25]
Ultraviolet divergences of quantum gravity	An effective-field-theory treatment or a new ultraviolet completion [26–30]

Table 1: Major unresolved problems of modern gravitational physics and the separate supplementary sectors or mechanisms commonly introduced to address them. Adapted from Ref. [7], with representative references to the corresponding conventional frameworks.

These conceptual limitations motivate a quantitative reexamination of the observable universe itself. In Sec. 2, we show that the observable universe can be locally low density and weak field while still having a globally important compactness and a non negligible GSE density. This prepares the ground for the central claim of the present paper: the same compactness condition that makes black hole interiors problematic for unmodified classical GR may also be relevant at the cosmological scale.

1.4 Definition of a Cosmological Black Hole and Aim of This Paper

In this paper, we use the term cosmological black hole to denote the Schwarzschild equivalent gravitational configuration associated with the matter-sector mass contained inside an observer-centered cosmological causal domain. For such a domain, the enclosed matter-sector mass $M(t)$, including baryonic matter and dark matter and excluding any independent dark energy component, defines the corresponding Schwarzschild-equivalent radius scale,

$$R_S(t) = \frac{2GM(t)}{c^2}. \tag{2}$$

This terminology does not mean that the entire universe is an isolated vacuum Schwarzschild black hole. It assigns a Schwarzschild-equivalent radius to the mass energy contained inside the chosen causal domain. Whether the causal radius $R_U(t)$ lies inside this radius, namely whether $R_U(t) < R_S(t)$, is a compactness condition to be evaluated for the observable universe. In this compactness sense, the present observable universe lies inside its own Schwarzschild-equivalent radius scale. The question of whether such a domain can later escape its Schwarzschild-equivalent event horizon is addressed in Sec. 6.5.4.

The purpose of this paper is to reformulate Black Hole Cosmology using total GSE dynamics. We argue that the three standard objections to BHC can be resolved within total GSE dynamics. The singularity is replaced, within this framework, by a finite radius structure characterized by R_{gs} and $R_{\min,BH}$ [7]. The objection based on the apparent absence of habitable interior regions is resolved in principle because sufficiently massive black hole interiors can contain macroscopic nonsingular domains, with a stable GSE radius R_{gs} that can exceed the size of the observable universe [5, 7]. The expansion problem is transformed from an objection into a cosmological signature of Black Hole Cosmology based on total GSE dynamics: in the cosmological application, the total GSE density appears as a dark energy density [6], and for $R_U < R_{\min,E}$ it becomes positive. When this positive component is large enough to satisfy the appropriate acceleration threshold, it carries negative pressure for $w_\Lambda \simeq -1$ and can drive accelerated expansion [6].

Finally, within the present framework, **the accelerated expansion of the universe is not evidence against Black Hole Cosmology; rather, it is interpreted as evidence for a total GSE based Black Hole Cosmology.** Thus, by deriving and testing the total GSE dark energy density equation against the observed dark energy density, this paper argues that Black Hole Cosmology can be made observationally testable [6].

2 The Incompleteness of Classical General Relativity in the Observable Universe

The preceding section explained why the standard objections to Black Hole Cosmology are not decisive when they rely only on the unmodified classical Schwarzschild interior [8,10,17]. The present section makes this point quantitative. The central observation is that a system can be locally low density and weak field, while still possessing a globally important compactness and a non negligible GSE density [6, 7]. Therefore, the usual weak field intuition is not sufficient for judging the gravitational state of the observable universe as a whole.

The discussion in this section uses the ordinary single term GSE as a diagnostic. The full total GSE dynamics will be introduced in the next section. The purpose here is more limited: to show that, even when only the conventional GSE term is considered, its mass-equivalent density can already exceed the mean matter density on the scale of the observable universe.

2.1 Failure of Both the Low Density Intuition and the Weak Field Intuition

The usual GSE of a self gravitating system has the form

$$U_{gs} = -\beta \frac{GM^2}{R}, \tag{3}$$

where β is a structural coefficient determined by the mass distribution. For a uniform Newtonian sphere, $\beta = 3/5$ [31]. In relativistic or astrophysical compact configurations, β is naturally of order unity [32, 33], and for a centrally concentrated classical $n = 3$ polytropic structure one has $\beta = 3/2$ [34].

Now consider the present observable universe with

$$R_U \simeq 46.5\,\mathrm{Gly}, \qquad \rho_m \simeq 2.68 \times 10^{-27}\,\mathrm{kg\,m^{-3}}, \tag{4}$$

where ρ_m denotes the mean matter density including baryonic matter and dark matter [15]. For a spherical causal domain of volume

$$V_U = \frac{4\pi}{3} R_U^3, \tag{5}$$

the enclosed matter mass is

$$M = \rho_m V_U. \tag{6}$$

The corresponding GSE density is obtained by dividing the mass equivalent of U_{gs} by the causal volume:

$$\rho_{gs} = \frac{U_{gs}}{c^2 V_U} = -\frac{4\pi\beta G}{3c^2} \rho_m^2 R_U^2. \tag{7}$$

For $\beta = 1$, this gives

$$\rho_{gs} \simeq -4.3 \times 10^{-27}\,\mathrm{kg\,m^{-3}}. \tag{8}$$

Therefore,

$$\rho_m : \rho_{gs} \simeq 1 : -1.62. \tag{9}$$

Thus, even though the observable universe is locally a low density and weak field system, the magnitude of its GSE density exceeds the matter density itself.

If the same observable volume is evaluated using the standard critical density [15]

$$\rho_c \simeq 8.52 \times 10^{-27}\,\mathrm{kg\,m^{-3}}, \tag{10}$$

then the corresponding single term GSE density becomes

$$\rho'_{gs} = -\frac{4\pi\beta G}{3c^2}\rho_c^2 R_U^2. \tag{11}$$

For $\beta = 1$, this gives

$$\rho'_{gs} \simeq -4.37 \times 10^{-26}\,\mathrm{kg\,m^{-3}}, \tag{12}$$

or

$$\rho_c : \rho'_{gs} \simeq 1 : -5.13. \tag{13}$$

If the Newtonian uniform sphere value $\beta = 3/5$ is used instead, the same estimate gives

$$\rho_c : \rho'_{gs} \simeq 1 : -3.08. \tag{14}$$

These estimates show that, on the cosmic horizon scale, GSE is not a negligible correction even in a low density and locally weak field universe [6, 7]. In this sense, the statement that gravity must reduce only to the Newtonian potential in a low density, weak field regime is incomplete. A system can remain locally weak field while its global gravitational self-energy is dynamically important. Contrary to the local weak field intuition, sufficiently large cosmic domains, including void like underdense regions when their characteristic scale is large enough, can retain a weak local gravitational field while the GSE contribution becomes comparable to or larger than the corresponding matter energy contribution.

2.2 The Observable Universe Satisfies the Black Hole Interior Compactness Condition

The same limitation of the weak field intuition appears in the compactness ratio of the observable universe. Taking the mean matter density, including baryonic matter and dark matter, as [15]

$$\rho_m \simeq 2.68 \times 10^{-27}\,\mathrm{kg\,m^{-3}}, \tag{15}$$

the matter only Schwarzschild-equivalent radius of the present observable universe is approximately

$$R_S \simeq 150.4\,\mathrm{Gly}. \tag{16}$$

Since the observable universe causal radius is

$$R_U \simeq 46.5\,\mathrm{Gly}, \tag{17}$$

one obtains

$$\frac{R_S}{R_U} \approx \frac{150.4\,\mathrm{Gly}}{46.5\,\mathrm{Gly}} \approx 3.23 > 1. \tag{18}$$

Thus, even in low density and locally weak field situations, one can have a globally high compactness configuration with $R_S/R_U > 1$ [7, 15].

As a comparison scale, if the same observable volume is evaluated using the standard critical density ρ_c [15], the corresponding Schwarzschild-equivalent radius becomes approximately

$$R_{S,c} \simeq 477\,\mathrm{Gly}, \tag{19}$$

giving

$$\frac{R_{S,c}}{R_U} \approx \frac{477\,\mathrm{Gly}}{46.5\,\mathrm{Gly}} \approx 10.3 > 1. \tag{20}$$

Therefore, the conclusion $R_S/R_U > 1$ is not a marginal result of the matter only estimate; it becomes even stronger when the critical density scale is used.

When the compactness ratio is used as the diagnostic quantity, the observable universe lies in a region satisfying

$$R_U < R_S, \tag{21}$$

which corresponds to the compactness condition of a black hole interior. Classical general relativity predicts a singularity at the endpoint of black hole collapse, where the classical description itself loses its physical applicability. Wald explicitly describes the prediction of singularities as a "breakdown of general relativity", because the classical description cannot be expected to remain valid near a spacetime singularity [17, p. 212]. This singularity prediction is therefore a direct signal that the unmodified classical theory is not a complete description of black hole interiors.

If General Relativity is incomplete inside a black hole,
then it is also incomplete in the observable universe.

Its incompleteness requires an inflaton field and dark energy.

This statement does not mean that the entire universe is an isolated vacuum Schwarzschild black hole. It means that the observable universe satisfies the same high compactness condition that makes the classical black hole interior problematic. Therefore, using a theoretical framework that is incomplete inside black holes as a decisive argument against Black Hole Cosmology contains an internal limitation. In this view, the dark energy sector can be interpreted as a manifestation of a missing gravitational principle required for a cosmic domain with black hole interior compactness [6].

This motivates the total GSE framework developed in the following sections [6, 7].

2.3 Spherical-Domain Compactness in an FLRW Universe

The assignment of a Schwarzschild-equivalent radius to an observer-centered cosmological domain does not replace the FLRW metric with the Schwarzschild vacuum metric. The cosmological background remains homogeneous and isotropic, and its evolution is governed by the Friedmann equations. The quantity

$$R_S(R) = \frac{2GM(R)}{c^2}$$

is used here as the gravitational-radius scale associated with the mass enclosed inside a spherical domain of areal radius R.

For a homogeneous and isotropic cosmic fluid, consider a comoving spherical domain whose physical radius is

$$R(t) = a(t)\chi.$$

Its radial acceleration follows directly from the Friedmann acceleration equation,

$$\frac{d^2R}{dt^2} = -\frac{4\pi G}{3}\left(\rho + \frac{3P}{c^2}\right)R. \tag{22}$$

Thus, **the radial evolution of the spherical domain is determined by the density and pressure of the fluid within the shell.** Carroll and Ostlie summarize this spherical-domain result as follows:

> $$\frac{d^2R}{dt^2} = -\frac{4\pi G}{3}\left(\rho + \frac{3P}{c^2}\right)R. \tag{29.51}$$
>
> Equation (29.51) is an illustration of **Birkhoff's theorem**. In 1923 the American mathematician G. D. Birkhoff (1884–1944) proved quite generally that for a spherically symmetric distribution of matter, Einstein's field equations have a unique solution. As a corollary, the acceleration of an expanding shell in our fluid universe is determined solely by the fluid lying within the shell. Equation (29.51) shows that the acceleration does not depend on any factors other than ρ, P, and R. Because Birkhoff's theorem holds even when general relativity is included, it is quite important in the study of cosmology [35].

Strictly, Birkhoff's theorem applies to spherically symmetric vacuum regions. In a cosmological fluid, the corresponding argument is more precisely described as shell theorem or Birkhoff-type spherical reasoning, together with the Misner–Sharp quasi-local mass in spherical symmetry. The continuation of the same homogeneous matter distribution outside the selected sphere does not introduce an additional independent radial force term into Eq. (22). The gravitational evolution of the chosen spherical domain is expressed in terms of its enclosed energy density, pressure, and quasi-local mass.

For the matter sector inside a homogeneous spherical domain, the enclosed mass is

$$M_m(R) = \frac{4\pi}{3}\rho_m R^3. \tag{23}$$

The corresponding dimensionless matter-sector compactness is therefore

$$\mathcal{C}_m(R) \equiv \frac{2GM_m(R)}{c^2R} = \frac{R_{S,m}(R)}{R} = \frac{8\pi G}{3c^2}\rho_m R^2. \tag{24}$$

Equation (24) is a quasi-local compactness diagnostic. It does not assert that the interior metric of the cosmological domain is the Schwarzschild vacuum metric.

For the present observable causal domain,

$$R_U \simeq 46.5 \text{ Gly}, \qquad R_{S,m} \simeq 150.4 \text{ Gly}, \tag{25}$$

and hence

$$\mathcal{C}_m(R_U) = \frac{R_{S,m}}{R_U} \simeq \frac{150.4 \text{ Gly}}{46.5 \text{ Gly}} \simeq 3.23 > 1. \tag{26}$$

This result states that the matter-sector mass enclosed inside the observable causal domain defines a Schwarzschild-equivalent gravitational radius larger than the causal radius itself. A very low local matter density therefore does not imply a small gravitational compactness when the causal domain is sufficiently large.

The present framework identifies this high-compactness causal domain as a cosmological black hole after its dynamics is completed by the total GSE contribution. The claim is therefore based on the combination of the quasi-local condition

$$R_U < R_{S,m}$$

and the total-GSE-completed cosmological dynamics. It does not arise from substituting the Schwarzschild vacuum metric for the FLRW metric, nor does it require the entire universe to be a finite isolated black hole surrounded by vacuum.

3 Total GSE Dynamics and Repulsive Gravity

3.1 From Conventional GSE to Total GSE

In the earlier GSE based approach to Black Hole Cosmology [5], the GSE of a self gravitating spherical configuration was represented by the familiar attractive binding term,

$$U_{gs}(R) = -\beta \frac{GM_{fr}^2}{R}, \tag{27}$$

where M_{fr} denotes the free state mass and β is a structural coefficient determined by the mass distribution. For a uniform Newtonian sphere, $\beta = 3/5$ [31].

Equation (27) captures the negative binding energy contribution of a self gravitating system. In general relativity, however, gravitational sourcing is not limited to rest mass energy alone [8, 17]. At the system level or quasi local level, gravitational binding energy contributes to the mass energy bookkeeping of a self gravitating configuration [8, 36, 37]. As part of this system level mass energy budget, the GSE contribution modifies the effective gravitational source rather than remaining a passive external binding term. When this source complete bookkeeping is applied to a self gravitating sphere, the ordinary single attractive GSE term is completed by the matter–GSE interaction term, yielding the two term total GSE functional [6, 7, 38].

3.2 Effective Source and the Origin of the Interaction Term

The physical origin of the second term can be understood from the effective source viewpoint [6]. For a self gravitating configuration, the source should not be identified only with the free state matter mass. The gravitational binding energy also contributes to the total mass energy budget of the bound system [8, 36]. If the GSE of the interior region is written as

$$U_{gs}(r) = -\beta \frac{GM'(r)^2}{r}, \tag{28}$$

then its signed equivalent mass contribution is

$$\frac{U_{gs}(r)}{c^2} = -\beta \frac{GM'(r)^2}{rc^2}. \tag{29}$$

For later convenience, we define the positive magnitude of this equivalent mass of GSE as

$$M'_{gs}(r) = \frac{|U_{gs}(r)|}{c^2} = \beta \frac{GM'(r)^2}{rc^2}. \tag{30}$$

The effective interior source is therefore written as the free matter mass plus the signed GSE contribution,

$$M_{\text{eff}}(r) = M'(r) + \frac{U_{gs}(r)}{c^2} = M'(r) - M'_{gs}(r). \tag{31}$$

This form makes explicit that the GSE is included additively in the mass-energy bookkeeping, while its negative sign reduces the effective source relative to the free-state matter mass.

Applying this effective source bookkeeping to the gravitational binding energy integral leads to the total GSE form in Eq. (32) [6]. The positive second term in Eq. (32) arises as the matter–GSE interaction energy contribution within the source completed bookkeeping of the self gravitating system.

The total GSE used in the present work is

$$\boxed{U_{gs-T}(R) = -\beta\frac{GM_{fr}^2}{R}\left(1 - \frac{5\beta}{7}\frac{GM_{fr}}{c^2R}\right)} \tag{32}$$

or equivalently,

$$U_{gs-T}(R) = -\beta\frac{GM_{fr}^2}{R} + \frac{5}{7}\beta^2\frac{G^2M_{fr}^3}{c^2R^2}. \tag{33}$$

The derivation of this total GSE functional from the equivalent gravitational source bookkeeping is summarized in Appendix A.

When Eq. (32) is expanded, the first contribution is the ordinary attractive GSE term. The positive second contribution is the matter–GSE interaction energy term, arising from the fact that the GSE contribution enters the effective mass energy bookkeeping of the self gravitating system. In this sense, the total GSE functional contains both the attractive gravitational binding contribution and the positive energy contribution responsible for the repulsive radial response.

This two term structure is central to the present paper. In the weak compactness regime, the second term is negligible and the ordinary attractive GSE term is recovered. In the high compactness regime, however, the second term grows faster because it scales as R^{-2}. Therefore, the total GSE dynamics differs qualitatively from the conventional single term picture near the Schwarzschild scale [7].

3.3 Total GSE Radial Dynamics

The total GSE dynamics is obtained by taking the radial derivative of the total GSE functional. For the collective radial mode of a self gravitating configuration, we write

$$D_T U = -\frac{1}{M_{fr}}\frac{dU_{gs-T}}{dR}, \tag{34}$$

where R is the physical radius of the mass energy distribution and $U = D_T R$ is the proper radial velocity. This relation is used as the effective radial acceleration form of the total GSE dynamics [7].

Using Eq. (32), one obtains

$$\frac{dU_{gs-T}}{dR} = \beta\frac{GM_{fr}^2}{R^2} - \frac{10}{7}\beta^2\frac{G^2M_{fr}^3}{c^2R^3}. \tag{35}$$

Therefore,

$$D_T U = -\beta\frac{GM_{fr}}{R^2}\left[1 - \frac{5\beta}{7}\frac{R_S}{R}\right], \qquad R_S = \frac{2GM_{fr}}{c^2}. \tag{36}$$

This equation is the central dynamical relation of the present paper. It shows explicitly that the total GSE dynamics contains an attractive branch and a repulsive branch [7].

The transition occurs when the bracket in Eq. (36) vanishes:

$$1 - \frac{5\beta}{7}\frac{R_S}{R} = 0. \tag{37}$$

Solving this condition gives the **stable equilibrium radius**

$$\boxed{R_{gs} = \frac{5\beta}{7}R_S} \tag{38}$$

At this radius,

$$D_T U = 0. \tag{39}$$

Thus, R_{gs} is the equilibrium radius of the total GSE dynamics. The stability of this radius follows from the sign reversal of $D_T U$ on the two sides of R_{gs} [7].

3.4 Attractive and Repulsive Regimes

Equation (36) divides the radial dynamics into two regimes.

For

$$R > R_{gs}, \tag{40}$$

the bracket in Eq. (36) is positive, and therefore

$$D_T U < 0. \tag{41}$$

The radial acceleration is directed inward. In this regime, the attractive GSE term dominates, and the system behaves in the ordinary gravitationally attractive manner.

For

$$R < R_{gs}, \tag{42}$$

the bracket in Eq. (36) becomes negative, and therefore

$$D_T U > 0. \tag{43}$$

The radial acceleration is directed outward. In this regime, the matter–GSE interaction term dominates, and the system enters a repulsive gravitational regime. This repulsive response arises because the GSE contribution enters the effective source as a negative equivalent mass term, $U_{gs}/c^2 = -M'_{gs}$, so that its gravitational effect on positive matter is outward in the total GSE dynamics [7].

This sign reversal is the key physical mechanism of the present work. The total GSE dynamics does not extrapolate a self gravitating configuration toward the singular limit $R \to 0$. Instead, the inward attractive branch for $R > R_{gs}$ and the outward repulsive branch for $R < R_{gs}$ drive the system toward the stable equilibrium radius R_{gs}. Thus, the total GSE dynamics replaces the pointlike collapse limit by a finite radial stabilization mechanism [7].

4 Internal Structure of Black Holes

4.1 A Global Black Hole Need Not Be Locally Trapped Everywhere

One of the most common objections to Black Hole Cosmology is based on the intuitive image that everything inside a black hole must already be in a locally trapped black hole state. This intuition is often associated with the vacuum Schwarzschild black hole picture, although the Schwarzschild geometry is a vacuum solution and cannot by itself describe a matter-filled interior region [8, 10, 17]. This intuition is misleading for a realistic gravitational collapse or for a cosmic mass distribution. The interior region is filled with matter and energy, and in the spherical-domain description its local physical state is governed by the mass-energy enclosed inside each spherical domain, not by the total mass of the entire configuration [8, 37].

The key observation was already introduced in the earlier discussion of the problems and solutions of Black Hole Cosmology [5]. Consider, for analytical clarity, a uniform spherical

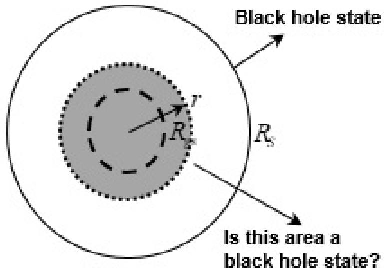

Figure 1: **When a macroscopic black hole is formed, an inner mass sphere of radius $r < R_S$ is not automatically in a local black hole compactness condition [5].** Consequently, during the gravitational contraction process, the interior mass distribution can continue to undergo physical processes such as virialization and energy emission [5, 10].

mass distribution of total free-state mass M_{fr} whose global radius has reached its Schwarzschild radius,

$$R = R_S, \qquad R_S = \frac{2GM_{fr}}{c^2}. \tag{44}$$

The whole configuration is then globally at the black hole compactness condition. Now consider an inner spherical region of radius r, where $0 < r < R_S$. The mass enclosed inside this region is

$$M(r) = \frac{4\pi}{3} r^3 \rho = M_{fr} \left(\frac{r}{R_S}\right)^3. \tag{45}$$

The Schwarzschild equivalent radius associated with this enclosed mass is

$$R_{S,M(r)} = \frac{2GM(r)}{c^2} = R_S \left(\frac{r}{R_S}\right)^3. \tag{46}$$

This can be rewritten as

$$R_{S,M(r)} = r \left(\frac{r}{R_S}\right)^2. \tag{47}$$

Since $r < R_S$, one has

$$\left(\frac{r}{R_S}\right)^2 < 1, \tag{48}$$

and therefore

$$R_{S,M(r)} < r. \tag{49}$$

Equation (49) states that the inner mass sphere of radius r lies outside the Schwarzschild equivalent radius generated by its own enclosed mass. Thus, even when the whole mass distribution satisfies the global black hole condition, an inner mass sphere is not automatically in a local black hole compactness condition [5]. For example, the mass enclosed inside the sphere $r = R_S/2$ has the Schwarzschild equivalent radius

$$R_{S,M(R_S/2)} = \frac{1}{8} R_S. \tag{50}$$

The radius of this inner region is $R_S/2$, while its own gravitational radius is only $R_S/8$. For this inner region to become an independent local black hole, it must be compressed by an additional factor of four in radius, corresponding to a density increase by a factor of $4^3 = 64$ [5].

This local-domain result changes the starting point for Black Hole Cosmology. A cosmic black hole configuration does not imply that every local region inside it is already a singular or locally trapped object. The interior can contain ordinary matter-filled regions that undergo physical evolution. This opens the possibility that a sufficiently large black hole scale universe can possess a broad interior region with weak local curvature, large-scale structure formation, and approximately flat cosmological geometry [5].

4.2 Matter-Filled Interior and Total GSE Dynamics

The previous subsection addresses the local physical state of the interior. The next question is the final fate of the collapsing or self-gravitating matter distribution. In the standard idealized picture, a pressureless matter distribution can collapse toward $R = 0$ [9, 11, 17]. In the total GSE dynamics, the pointlike endpoint is replaced by a finite radial energy landscape [7].

The total GSE of a self-gravitating configuration is

$$U_{gs-T}(R) = -\beta \frac{GM_{fr}^2}{R} + \frac{5}{7}\beta^2 \frac{G^2 M_{fr}^3}{c^2 R^2}. \tag{51}$$

The first term is the attractive GSE term. The positive second term arises as the matter–GSE interaction contribution generated when the signed GSE equivalent mass is included in the effective source bookkeeping of the self-gravitating system [6, 7, 38]. The radial dynamics follows from the gradient of this total GSE functional: $D_T U = -\frac{1}{M_{fr}} \frac{dU_{gs-T}}{dR}$.

Using Eq. (51), one obtains

$$D_T U = -\beta \frac{GM_{fr}}{R^2} \left[1 - \frac{5\beta}{7} \frac{R_S}{R}\right]. \tag{52}$$

The acceleration vanishes at

$$R_{gs} = \frac{5\beta}{7} R_S. \tag{53}$$

For $R > R_{gs}$, the attractive branch dominates and $D_T U < 0$. For $R < R_{gs}$, the matter–GSE interaction term dominates and $D_T U > 0$. The radial acceleration is then directed outward. The total GSE dynamics therefore drives the configuration toward the stable equilibrium radius R_{gs} instead of toward the pointlike limit $R = 0$ [7].

The second characteristic scale is the **energy-limited minimum radius** $R_{\min,E}$. Using the free-state configuration at infinite separation as the zero of potential energy, it is defined by

$$U_{\mathrm{gs-T}}(R_{\min,E}) = 0\,. \tag{54}$$

Below this radius, the total GSE becomes positive, so further compression would require additional external energy. Solving this condition gives

$$\boxed{R_{\min,E} = \frac{5\beta}{14} R_S} \tag{55}$$

The third characteristic scale is the **black hole energy-limited radius** $R_{\min,BH}$. For a black hole formed when the collapsing mass distribution first reaches $R = R_S$, the available total GSE energy level of the matter-filled interior is constrained by the energy level at horizon formation:

$$U_{gs-T}(R_{\min,BH}) = U_{gs-T}(R_S). \tag{56}$$

Solving this condition gives

$$R_{\min,BH} = \frac{5\beta}{14 - 5\beta} R_S. \tag{57}$$

As the distribution contracts inward from R_S, the total GSE first decreases and reaches its minimum at R_{gs}. If the contraction proceeds further inward from R_{gs}, the total GSE increases again. Therefore, $R_{\min,BH}$ represents the limiting radius that can be reached using the energy available inside the black hole at the moment of horizon formation. Below $R_{\min,BH}$, further contraction would require additional energy beyond the energy trapped inside the black hole interior during its formation [7].

By contrast, $R_{\min,E}$ is the theoretical lower radius obtained when the free-state configuration at infinite separation is used as the zero of potential energy. It corresponds to the limiting case in which the entire initial free-state energy budget is available for compression. In a physically formed isolated black hole, however, the more relevant energy bound is generally $R_{\min,BH}$, because the energy available inside the black hole is fixed by the energy trapped at horizon formation [7].

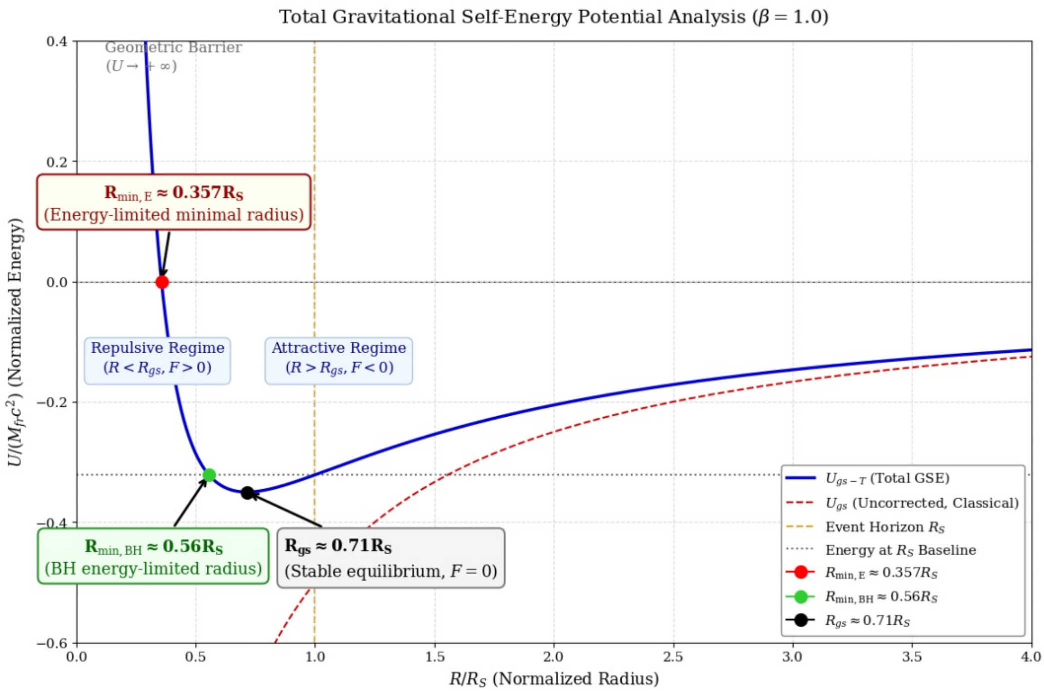

Figure 2: **Total GSE energy landscape for $\beta = 1$.** The curve has a minimum at $R_{gs} \simeq 0.714R_S$, where the radial acceleration vanishes. The energy-limited radii $R_{\min,BH} \simeq 0.556R_S$ and $R_{\min,E} \simeq 0.357R_S$ mark, respectively, the event horizon formation energy bound and the free-state zero energy bound. Within total GSE dynamics, these scales replace the singularity with a finite-radius structure characterized by finite physical radii [7].

For the representative case $\beta = 1$, these radii become

$$\boxed{R_{gs} = \frac{5}{7}R_S \simeq 0.714R_S}, \quad \boxed{R_{\min,BH} = \frac{5}{9}R_S \simeq 0.556R_S}, \quad \boxed{R_{\min,E} = \frac{5}{14}R_S \simeq 0.357R_S} \tag{58}$$

For $0 < \beta < 7/5$, the stable radius R_{gs} lies inside the global horizon. In this range, the total GSE dynamics describes a black hole with a finite nonsingular interior core. For $7/5 < \beta < 14/5$, the simplified homogeneous model places R_{gs} outside R_S, suggesting pre-horizon stabilization within this idealized estimate. In realistic collapse, rotation, pressure, nonuniform density, virialization, and energy redistribution can shift the effective structure coefficient and the detailed radius ordering. The essential point is that the total GSE energy landscape contains finite characteristic radii and removes the unbounded descent toward $R = 0$ [7].

4.3 Macroscopic Nonsingular Cores

The finite radii in Eq. (58) are proportional to the Schwarzschild radius of the mass-energy distribution. They are not necessarily microscopic or Planck-sized. For a stellar-mass black hole, R_S is measured in kilometers; hence R_{gs} and $R_{\min,BH}$ are also macroscopic. For a supermassive black hole, the same radii scale to astronomical sizes. For a cosmic black hole configuration, they can be larger than the observable universe [7].

For example, the matter content of the present observable universe, including baryonic matter and dark matter, gives a matter-only Schwarzschild equivalent radius

$$R_{S,m} \simeq 150.4\,\mathrm{Gly}, \tag{59}$$

whereas the present observable radius is

$$R_{\mathrm{obs}} \simeq 46.5\,\mathrm{Gly}. \tag{60}$$

Thus,

$$\frac{R_{S,m}}{R_{\mathrm{obs}}} \simeq \frac{150.4}{46.5} \simeq 3.23. \tag{61}$$

If the same observable volume is evaluated using the present critical density,

$$\rho_c = \frac{3H_0^2}{8\pi G} \simeq 8.53 \times 10^{-27}\,\mathrm{kg\,m^{-3}}, \tag{62}$$

then the corresponding critical density Schwarzschild equivalent radius becomes

$$R_{S,\mathrm{crit}} \simeq 477\,\mathrm{Gly}. \tag{63}$$

Therefore,

$$\frac{R_{S,\mathrm{crit}}}{R_{\mathrm{obs}}} \simeq \frac{477}{46.5} \simeq 10.3. \tag{64}$$

In this Schwarzschild equivalent compactness diagnostic, these estimates show that the observable universe lies inside the event horizon generated by its matter content and also inside the corresponding event horizon associated with the present critical density content [7].

This scaling is crucial for Black Hole Cosmology. The existence of a global black hole compactness condition does not force the interior to collapse into a point singularity. The interior mass distribution can be stabilized by the total GSE dynamics at a finite radius. In a cosmic configuration, the corresponding nonsingular interior region can in principle be large enough to contain an almost homogeneous and approximately flat observable universe [5, 7].

In the earlier single-term GSE formulation, the cancellation between positive mass energy and negative GSE suggested that a large nearly flat interior region could exist inside a sufficiently large black hole [5]. In the present total GSE formulation, the stabilizing structure is governed by the two-term energy landscape. The stable radius R_{gs} is determined by the vanishing of the total radial acceleration, while the energy-limited radii $R_{\min,E}$ and $R_{\min,BH}$ provide lower bounds on further contraction. Thus, the nonsingular interior is not introduced as a separate assumption; it follows from the finite-radius structure of the total GSE dynamics [7].

The purpose of this section is limited to the internal structure of black holes. The result is that total GSE dynamics replaces the point singularity with finite characteristic radii and allows a macroscopic nonsingular interior. The cosmological consequences of this finite-radius structure, including cosmic expansion and the total GSE interpretation of dark energy, will be discussed in the following sections.

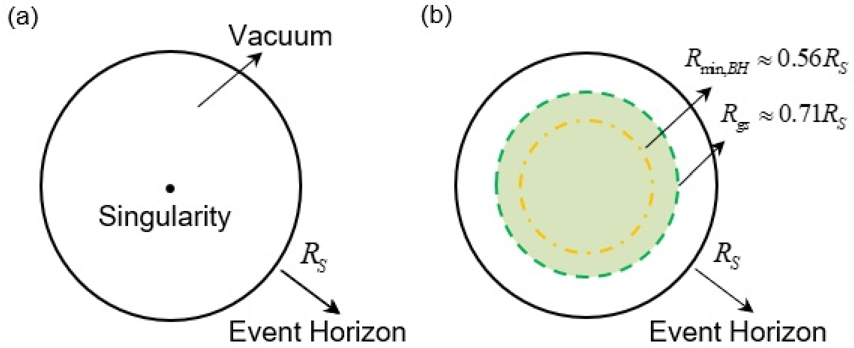

Figure 3: **Stable equilibrium radius R_{gs} and black hole energy-limited radius $R_{\min,BH}$ for $\beta = 1$.** Panel (a) represents the classical point singularity picture. Panel (b) shows the finite-radius interior structure in the total GSE dynamics. For a black hole with Schwarzschild radius R_S, the mass-energy distribution cannot be compressed below the corresponding black hole energy-limited radius $R_{\min,BH}$ using only the energy budget available at event horizon formation. If additional energy enters the black hole, the Schwarzschild radius is rescaled accordingly, and the limiting radius is also rescaled with the new value of R_S. After relaxation, the distribution is expected to settle near R_{gs}.

5 Cosmic Expansion in a Black Hole Universe

5.1 Cosmic Expansion and Total GSE Dark Energy Density

The third standard objection to Black Hole Cosmology is the expansion problem. The usual intuition associates the interior of a black hole with contraction toward a singularity, whereas the observed universe expands and is presently undergoing accelerated expansion [13–16]. In the present framework, we reformulate this objection by distinguishing the black hole interior use of total GSE from its cosmological use.

For an isolated stellar-type or closed black hole, the relevant variable is the radius of a finite self-gravitating mass distribution. In that case, the radial response follows from the gradient of the total GSE potential, $D_T U$. This gives an attractive branch for $R > R_{gs}$, a repulsive branch for $R < R_{gs}$, and a stable equilibrium radius R_{gs}. This is the finite-radius stabilization mechanism of the matter-filled black hole interior [7].

The cosmological use of total GSE is different. The universe is not a finite isolated object with a material surface whose radius is pushed directly by a force $-dU_{gs-T}/dR$. Cosmological dynamics instead treats the universe as an expanding spacetime background, and the relevant scale is the causal radius of the observable domain [12, 15]. This causal radius is not the surface of a fixed material body. It is a horizon scale that grows as the universe ages and as additional matter becomes causally connected to the observer. Therefore, in the cosmological application, we do not use total GSE as a direct force law for the motion of the horizon. In the cosmological interpretation, the total GSE density is identified as the dark energy density generated by the mass-energy contained inside the causal domain [6].

Let $R_U(t)$ denote the causal radius of the observable universe domain under consideration. In the present application, $R_U(t)$ may be identified with the physical particle horizon scale or, more generally, with the observer-centered causal horizon [12, 15]. It denotes the causal size of the observable domain, not the physical radius of the entire universe. Let $M(t)$ be the mass-energy enclosed inside this causal domain. The corresponding Schwarzschild-equivalent radius is $R_S(t) = \frac{2GM(t)}{c^2}$. When this Schwarzschild-equivalent radius exceeds the causal radius,

$R_U(t) < R_S(t)$, we call the corresponding causal domain a cosmological black hole in the sense defined in Sec. 1.4.

The total GSE associated with the mass-energy inside the causal domain is written as

$$U_{gs-T}(R_U, t) = -\beta \frac{GM(t)^2}{R_U}\left(1 - \frac{5\beta}{7}\frac{GM(t)}{c^2 R_U}\right). \tag{65}$$

In the cosmological interpretation, this total GSE gives a dark energy density after its mass-equivalent contribution is divided by the causal volume:

$$\rho_{\Lambda_m} = \frac{U_{gs-T}(R_U, t)}{c^2 V_c}, \qquad V_c = \frac{4\pi}{3} R_U^3. \tag{66}$$

Using

$$\rho_m = \frac{M(t)}{V_c}, \qquad R_S(t) = \frac{2GM(t)}{c^2}, \tag{67}$$

this gives

$$\rho_{\Lambda_m} = \frac{\beta \rho_m}{2}\frac{R_S}{R_U}\left(\frac{5\beta}{14}\frac{R_S}{R_U} - 1\right). \tag{68}$$

In this paper, the total GSE density is identified as the physical dark energy density generated by matter inside the causal domain. The word "effective" is reserved only for the fluid-level description in which this total GSE dark energy sector is represented by an equation-of-state parameter w_{Λ_m} and, if necessary, by an exchange term Q [6].

Equation (68) is the cosmological counterpart of the total GSE energy [6]. When

$$\rho_{\Lambda_m} < 0, \tag{69}$$

the total GSE contribution gives a negative contribution to the dark energy sector. When

$$\rho_{\Lambda_m} > 0, \tag{70}$$

it gives a positive dark energy density. The sign changes at

$$\rho_{\Lambda_m} = 0 \quad \Longleftrightarrow \quad \frac{R_S}{R_U} = \frac{14}{5\beta}. \tag{71}$$

Equivalently,

$$R_U = \frac{5\beta}{14} R_S = R_{\min,E}. \tag{72}$$

Thus, $R_{\min,E}$ is algebraically the zero of the total GSE energy. In the black hole interior problem, this radius has the meaning of an energy-limited lower radius for a fixed mass-energy system [7]. In cosmology, however, the enclosed mass $M(t)$ changes as the causal horizon grows. Therefore, we read Eq. (71) as an instantaneous compactness threshold for the sign of the dark energy density, not as a fixed energy lower bound on the causal radius.

5.2 The Cosmological Acceleration Threshold

A positive value of ρ_{Λ_m} is necessary for the total GSE sector to act as a dark energy component, but cosmic acceleration requires a stronger condition [15, 23]. Since ρ_{Λ_m} is generated by the total GSE of matter inside the causal domain, we treat it as a matter-induced dark energy sector rather than as an independent fundamental vacuum component [6]. In a general background description, the matter sector and the total GSE sector may exchange equivalent mass density.

We parametrize this exchange by a term Q. With this sign convention, we write the effective equation of state of the total GSE dark energy sector as

$$w_{\Lambda_m}(t) = -1 - \frac{\dot{\rho}_{\Lambda_m} + Q}{3H\rho_{\Lambda_m}}. \tag{73}$$

Here ($H \equiv \dot{a}/a$) is the Hubble parameter, i.e. the cosmic expansion rate, and (Q) parametrizes the effective exchange of equivalent mass density between the matter sector and the total GSE sector at the homogeneous background level. Therefore, (w_{Λ_m}) can generally depend on time [6, 23].

For the approximate cosmological dynamics considered in this paper, we adopt the dark energy limit

$$w_{\Lambda_m} \simeq -1, \tag{74}$$

and the late time regime of the MOC simulation also reproduces this behavior [6]. In this approximation,

$$p_{\Lambda_m} \simeq -\rho_{\Lambda_m} c^2. \tag{75}$$

For a matter component with negligible pressure and a total GSE dark energy component satisfying $w_{\Lambda_m} \simeq -1$, the acceleration condition becomes

$$\rho_{\Lambda_m} > \frac{1}{2}\rho_m. \tag{76}$$

Substituting Eq. (68) into Eq. (76) gives

$$\frac{\beta}{2}\frac{R_S}{R_U}\left(\frac{5\beta}{14}\frac{R_S}{R_U} - 1\right) > \frac{1}{2}. \tag{77}$$

The equality condition defines the cosmological acceleration threshold:

$$\frac{\beta}{2}\frac{R_S}{R_{\text{crit,U}}}\left(\frac{5\beta}{14}\frac{R_S}{R_{\text{crit,U}}} - 1\right) = \frac{1}{2}. \tag{78}$$

Solving this equation gives

$$R_{\text{crit,U}} = \frac{5\beta}{7\left(1+\sqrt{17/7}\right)} R_S \simeq 0.279\,\beta R_S. \tag{79}$$

Therefore, the two regimes are

$$R_U > R_{\text{crit,U}} \quad \Longrightarrow \quad \rho_{\Lambda_m} < \frac{1}{2}\rho_m \quad \Longrightarrow \quad \text{decelerating expansion,} \tag{80}$$

and

$$R_U < R_{\text{crit,U}} \quad \Longrightarrow \quad \rho_{\Lambda_m} > \frac{1}{2}\rho_m \quad \Longrightarrow \quad \text{accelerated expansion.} \tag{81}$$

The acceleration threshold lies below $R_{\min,E}$. Indeed,

$$\frac{R_{\text{crit,U}}}{R_{\min,E}} = \frac{2}{1+\sqrt{17/7}} \simeq 0.782, \qquad R_{\text{crit,U}} \simeq 0.782 R_{\min,E} < R_{\min,E}. \tag{82}$$

This creates no contradiction in the cosmological setting. The radius $R_{\min,E}$ was defined for a fixed mass-energy system whose energy is measured relative to a free-state configuration at infinite separation. The observable universe does not form by bringing a fixed set of particles from infinite separation into a fixed volume. Instead, as the universe ages, the causal horizon expands and new matter enters the gravitationally connected domain. Consequently, $M(t)$, $R_S(t)$, and $U_{gs-T}(t)$ change with time, and the total energy inside the causal domain is not a fixed conserved quantity [6].

For this reason, we express the cosmological acceleration criterion as an instantaneous condition involving $R_U(t)$, $R_S(t)$, and $R_{\text{crit,U}}(t)$, rather than as a fixed energy lower bound. The sign and acceleration regimes can be summarized as

$$R_U > R_{\min,E} \implies \rho_{\Lambda_m} < 0, \tag{83}$$

$$R_{\text{crit,U}} < R_U < R_{\min,E} \implies \rho_{\Lambda_m} > 0 \quad \text{but no accelerated expansion,} \tag{84}$$

$$R_U < R_{\text{crit,U}} \implies \rho_{\Lambda_m} > \frac{1}{2}\rho_m \quad \text{and accelerated expansion.} \tag{85}$$

Thus, the present framework does not describe cosmic acceleration as the direct radial force law of a black hole interior. Instead, cosmic acceleration arises when the total GSE of the causal domain gives a sufficiently large positive dark energy density, whose negative pressure drives accelerated expansion. This distinction will be essential in the following discussion of the observed dark energy density [6].

5.3 Early Accelerated Expansion and the GSE Inflation Trigger

The preceding subsections show that the total GSE of a causal cosmic domain defines the total GSE dark energy density. The inflationary calculation in this subsection follows the earlier MOC cosmology analysis and adapts it to the present Black Hole Cosmology framework [6]. It shows that the same total GSE dark energy density can reach the characteristic time and energy density scales usually associated with the standard inflationary epoch [18–20, 39].

In this section, $R_U(t)$ denotes the causal radius of the early observable universe domain. We identify it with the physical particle horizon scale, or more generally with the observer-centered causal horizon scale, in the order-of-magnitude estimate [12, 15]. Thus, $R_U(t)$ is not the physical radius of a finite isolated object, but the causal radius of the radiation relevant to the early-universe calculation.

In the early universe, the relevant question is whether the total GSE density (dark energy density) becomes large enough to dominate over the radiation component and produce negative-pressure-driven acceleration [6].

Near the Planck-scale trigger estimate, the relevant causal and physical length scales are not expected to possess a large hierarchy. Therefore, for the Planck-scale order of magnitude estimate, we take the physical particle horizon scale, the characteristic physical scale of the causally connected radiation domain, and the causal radius (R_U) to be of the same order:

$$R_{p,\text{phys}}(t) = a(t)\chi_p(t) \sim R_{\text{phys}}(t) \sim R_U(t). \tag{86}$$

This relation is not used as an exact horizon identity. It only states that, near the Planck-scale trigger estimate, no large hierarchy is assumed among the relevant causal and physical length scales.

Taking

$$\rho_r \simeq \rho_{\text{pl}}, \qquad R_U \simeq l_{\text{pl}}, \tag{87}$$

the compactness ratio becomes

$$\frac{R_S}{R_U} = \frac{2GM}{c^2 R_U} = \frac{2G\left(\frac{4\pi}{3}R_U^3\rho_{\text{pl}}\right)}{c^2 R_U} = \frac{8\pi G\rho_{\text{pl}} l_{\text{pl}}^2}{3c^2} = \frac{8\pi}{3} \simeq 8.38. \tag{88}$$

More generally,

$$\frac{R_S}{R_U} = \frac{8\pi}{3}\left(\frac{\rho_r}{\rho_{\rm pl}}\right)\left(\frac{R_U}{l_{\rm pl}}\right)^2. \tag{89}$$

Thus, the numerical value $R_S/R_U \simeq 8.38$ follows from the specific Planck-scale normalization $\rho_r \simeq \rho_{\rm pl}$ and $R_U \simeq l_{\rm pl}$. If a different causal radius or a different early radiation density is chosen, the numerical coefficient changes by the factor $(\rho_r/\rho_{\rm pl})(R_U/l_{\rm pl})^2$. The qualitative point is not the exact number 8.38, but the fact that a Planck-density causal domain with Planck-scale radius naturally has order-unity or larger compactness [6].

For the illustrative high compactness value $\beta \simeq 2$, the total GSE dark energy density becomes

$$\rho_{\Lambda_m} \simeq \frac{2\rho_{\rm pl}}{2}(8.38)\left[\frac{5(2)}{14}(8.38)-1\right] \simeq 41.8\,\rho_{\rm pl}. \tag{90}$$

Thus, at the Planck scale high-density limit, the total GSE dark energy density can greatly exceed the radiation density. This provides a compactness-driven route to an inflationary accelerated phase. The value $\beta \simeq 2$ is used here only as an illustrative high compactness estimate; even smaller values of β can already give $\rho_{\Lambda_m} > \rho_r$.

For comparison, even for the conservative value $\beta = 1$, the same Planck-scale compactness gives

$$\rho_{\Lambda_m} \simeq \frac{\rho_{\rm pl}}{2}(8.38)\left[\frac{5}{14}(8.38)-1\right] \simeq 8.34\,\rho_{\rm pl}. \tag{91}$$

Thus, the total GSE dark energy density still exceeds the radiation density by more than an order-one factor, so the condition for accelerated expansion is already satisfied in this estimate.

We use the Friedmann acceleration equation as a diagnostic relation,

$$\frac{\ddot{a}}{a} = -\frac{4\pi G}{3}\sum_i\left(\rho_i + \frac{3p_i}{c^2}\right). \tag{92}$$

For radiation,

$$p_r = \frac{1}{3}\rho_r c^2, \qquad \rho_r + \frac{3p_r}{c^2} = 2\rho_r. \tag{93}$$

For the total GSE dark energy during the accelerated background phase, we use the background level equation of state

$$p_{\Lambda_m} \simeq -\rho_{\Lambda_m} c^2, \qquad \rho_{\Lambda_m} + \frac{3p_{\Lambda_m}}{c^2} \simeq -2\rho_{\Lambda_m}. \tag{94}$$

Therefore,

$$\frac{\ddot{a}}{a} \simeq -\frac{8\pi G}{3}\left(\rho_r - \rho_{\Lambda_m}\right). \tag{95}$$

This vacuum-like approximation follows the standard background-level logic of inflationary cosmology, in which accelerated expansion is driven by an approximately constant energy density and the background is close to de Sitter expansion [18–20, 39]. In the old-inflation picture, this role is played by a false-vacuum energy density [18], whereas in conventional single-field slow-roll inflation it is realized by a scalar field whose potential energy dominates over its kinetic energy [19, 20]. The Starobinsky model provides a curvature-driven quasi-de Sitter realization, which can also be represented in an Einstein-frame scalaron description [39].

In conventional single-field slow-roll inflation, the inflaton energy density and pressure are

$$\rho_\phi = \frac{1}{2}\dot{\phi}^2 + V(\phi), \qquad p_\phi = \frac{1}{2}\dot{\phi}^2 - V(\phi). \tag{96}$$

When the potential energy dominates over the kinetic energy, $\dot{\phi}^2/2 \ll V(\phi)$, one obtains

$$\rho_\phi \simeq V(\phi), \qquad p_\phi \simeq -V(\phi), \qquad w_\phi \simeq -1. \tag{97}$$

Thus, the energy density remains nearly constant over a Hubble time and the expansion is quasi-de Sitter.

In the present framework, we use the same background-level logic as a fiducial approximation: during the early accelerated phase, the positive total GSE density is represented as a vacuum-like effective fluid with

$$p_{\Lambda_m} \simeq -\rho_{\Lambda_m} c^2. \tag{98}$$

This does not constitute a full perturbation-level derivation of the total GSE stress tensor. It is used here as a background-level trigger estimate for the onset of accelerated expansion.

The onset condition for accelerated expansion is

$$\rho_{\Lambda_m} > \rho_r, \tag{99}$$

with the threshold condition

$$\rho_{\Lambda_m} = \rho_r. \tag{100}$$

For the trigger estimate, we use the order of magnitude causal relation

$$\chi_p \simeq R_{\rm phys} \simeq R_U, \qquad R_U \simeq ct. \tag{101}$$

In this causal regime, the total GSE dark energy density can be written as

$$\rho_{\Lambda_m} = \frac{\beta \rho_r}{2} \frac{R_S}{R_U} \left(\frac{5\beta}{14} \frac{R_S}{R_U} - 1 \right), \tag{102}$$

where

$$R_S = \frac{2GM}{c^2}, \qquad M = \frac{4\pi}{3} R_U^3 \rho_r. \tag{103}$$

Dividing Eq. (102) by ρ_r gives

$$\frac{\rho_{\Lambda_m}}{\rho_r} = \frac{\beta}{2} \frac{R_S}{R_U} \left(\frac{5\beta}{14} \frac{R_S}{R_U} - 1 \right). \tag{104}$$

Using Eq. (103), the compactness ratio is

$$\frac{R_S}{R_U} = \frac{2GM}{c^2 R_U} = \frac{8\pi G}{3} \frac{R_U^2 \rho_r}{c^2}. \tag{105}$$

With $R_U \simeq ct$, this reduces to

$$\frac{R_S}{R_U} \simeq \frac{8\pi G}{3} t^2 \rho_r. \tag{106}$$

Substituting Eq. (106) into Eq. (104) gives the general β-dependent expression

$$\frac{\rho_{\Lambda_m}}{\rho_r} \simeq \frac{4\pi\beta G}{3} t^2 \rho_r \left(\frac{20\pi\beta G}{21} t^2 \rho_r - 1 \right). \tag{107}$$

The onset threshold for early accelerated expansion is

$$\rho_{\Lambda_m} = \rho_r. \tag{108}$$

Using Eq. (107), this condition gives

$$\frac{4\pi\beta G}{3}t^2\rho_r\left(\frac{20\pi\beta G}{21}t^2\rho_r-1\right)=1. \tag{109}$$

Equivalently,

$$\frac{80\pi^2\beta^2G^2}{63}\left(t^2\rho_r\right)^2-\frac{4\pi\beta G}{3}\left(t^2\rho_r\right)-1=0. \tag{110}$$

The physically relevant positive solution is

$$\boxed{t^2\rho_r=\frac{21}{40\pi G\beta}\left(1+\sqrt{\frac{27}{7}}\right)} \tag{111}$$

For the illustrative early high compactness estimate $\beta\simeq 2$, this becomes

$$t^2\rho_r\simeq\frac{21}{80\pi G}\left(1+\sqrt{\frac{27}{7}}\right)\simeq 3.71\times10^9\ \mathrm{kg,s^2,m^{-3}}. \tag{112}$$

This trigger relation gives a direct mapping between the onset time of early accelerated expansion and the required radiation density. If accelerated expansion begins at

$$t\simeq10^{-36}\,\mathrm{s}, \tag{113}$$

then

$$\rho_r(t\simeq10^{-36}\,\mathrm{s})\simeq3.71\times10^{81}\,\mathrm{kg\,m^{-3}}. \tag{114}$$

If one considers a later onset time,

$$t\simeq10^{-35}\,\mathrm{s}, \tag{115}$$

the required density decreases as t^{-2}, giving

$$\rho_r(t\simeq10^{-35}\,\mathrm{s})\simeq3.71\times10^{79}\,\mathrm{kg\,m^{-3}}. \tag{116}$$

Conversely, if the early universe has a nearly homogeneous radiation density of order

$$\rho_r\sim10^{79}\text{–}10^{81}\,\mathrm{kg\,m^{-3}}, \tag{117}$$

then the total GSE trigger condition is reached at $t\sim10^{-35}$–10^{-36} s.

This establishes the role of total GSE in the early accelerated phase. Inflation is not introduced here as an independent scalar field sector. It emerges, at the background level, when the compactness of the causally connected radiation domain makes ρ_{Λ_m} comparable to or larger than ρ_r. The present argument is an order of magnitude trigger estimate, not a full perturbation-level inflation model. The result shows that the time and energy density scales estimated from total GSE dynamics are in approximate agreement with the characteristic scales usually associated with standard inflation [18–20,39], supporting the interpretation that total GSE can provide the physical driving mechanism for the inflationary phase [6].

5.4 Transition from Early Acceleration to Decelerating Expansion

The total GSE inflation trigger is self-terminating at the background level. The same compactness factor that generates a large positive ρ_{Λ_m} at very early times decreases as the causal domain expands. Therefore, the early accelerated phase does not require a separate external exit mechanism in the background dynamics [6].

The sign and magnitude of the total GSE dark energy density are controlled by the factor

$$\Gamma(R_U) \equiv \left(\frac{5\beta}{14}\frac{R_S}{R_U} - 1\right), \tag{118}$$

which appears in

$$\rho_{\Lambda_m} = \frac{\beta \rho_r}{2}\frac{R_S}{R_U}\Gamma(R_U). \tag{119}$$

Using $M = \frac{4\pi}{3}R_U^3\rho_r$, $R_S = \frac{2GM}{c^2}$, the factor $\Gamma(R_U)$ can be rewritten as

$$\Gamma(R_U) = \left(\frac{20\pi\beta G}{21c^2}\rho_r R_U^2 - 1\right). \tag{120}$$

During the early radiation-dominated phase, the radiation density scales approximately as

$$\rho_r(R_U) = \rho_i\left(\frac{R_{U,i}}{R_U}\right)^4. \tag{121}$$

Substituting this into Eq. (120) gives

$$\Gamma(R_U) = \left[\frac{20\pi\beta G}{21c^2}\rho_i R_{U,i}^4\frac{1}{R_U^2} - 1\right] \equiv \left(\frac{C}{R_U^2} - 1\right), \tag{122}$$

where $C > 0$ is fixed by the initial conditions. This expression shows the self-terminating character of the mechanism. At extremely small R_U, the first term is large, $\Gamma(R_U) > 0$, and the total GSE dark energy density is positive. If $\rho_{\Lambda_m} > \rho_r$, the acceleration equation gives

$$\frac{\ddot{a}}{a} > 0, \tag{123}$$

and the universe enters an inflationary accelerated phase.

As the accelerated expansion proceeds, however, the same expansion increases the causal scale R_U. Since the leading contribution to $\Gamma(R_U)$ scales as R_U^{-2}, the positive total GSE contribution weakens automatically. The accelerated phase ends when the total GSE dark energy density drops below the radiation density. The approximate exit condition is therefore

$$\rho_{\Lambda_m} = \rho_r. \tag{124}$$

After this point,

$$\rho_{\Lambda_m} < \rho_r, \tag{125}$$

and the radiation term dominates the acceleration equation,

$$\frac{\ddot{a}}{a} \simeq -\frac{8\pi G}{3}\left(\rho_r - \rho_{\Lambda_m}\right) < 0. \tag{126}$$

The universe then enters a decelerating radiation-dominated expansion era.

There is also a later sign-change threshold,

$$\Gamma(R_U) = 0 \quad \Longleftrightarrow \quad \rho_{\Lambda_m} = 0. \tag{127}$$

Beyond this point, the total GSE dark energy density becomes negative. The end of accelerated expansion, however, occurs earlier, when ρ_{Λ_m} falls below the dominant radiation density. Thus, the graceful exit from the early accelerated phase is governed by the weakening of the same total GSE dark energy term that initiated inflation.

This gives the qualitative sequence

$$\rho_{\Lambda_m} > \rho_r \quad \Longrightarrow \quad \text{early accelerated expansion: inflation,} \tag{128}$$

$$0 < \rho_{\Lambda_m} < \rho_r \quad \Longrightarrow \quad \text{radiation-dominated decelerating expansion,} \tag{129}$$

$$\rho_{\Lambda_m} < 0 \quad \Longrightarrow \quad \text{attractive total GSE contribution.} \tag{130}$$

In this way, the transition from early acceleration to decelerating expansion follows from the expansion of the causal domain itself. The exit from the accelerated background phase is not a separate sector added by hand; it follows from the scale dependence of the total GSE dark energy density [6]. A detailed thermalization or reheating analogue is a separate problem and lies beyond the scope of this subsection.

5.5 Late-Time Acceleration from Causal Horizon Mass Growth

After the early accelerated phase ends, the universe enters a decelerating expansion era. This period includes the radiation era and the subsequent matter-dominated era [12, 15]. In the present framework, this middle epoch corresponds to a regime in which the total GSE dark energy density is either negative or too small to dominate the ordinary matter and radiation components. When $\rho_{\Lambda_m} < 0$, the total GSE contribution acts as an attractive contribution in the acceleration equation, and it supports the formation and growth of galaxies and large-scale cosmic structures rather than driving accelerated expansion [6].

This attractive total GSE phase provides a natural pathway for enhanced early structure growth. Since the negative total GSE density acts in the attractive direction during the intermediate decelerating epoch, it can increase the efficiency of early gravitational assembly without invoking an additional dark sector. This may help alleviate several early-structure tensions, including the rapid assembly of massive galaxies reported by JWST [40, 41] and the tensions in structure growth indicated by KiDS, and related surveys [42].

The transition to late-time accelerated expansion arises when the total GSE density acts as the positive dark energy density:

$$\rho_{\Lambda_m} = \frac{\beta \rho_m}{2}\frac{R_S}{R_U}\left(\frac{5\beta}{14}\frac{R_S}{R_U} - 1\right). \tag{131}$$

The relevant cosmological scale is now the causal radius $R_U(t)$, not the physical surface of a fixed isolated object. The enclosed mass changes with time:

$$R_S(t) = \frac{2GM(t)}{c^2}. \tag{132}$$

As the universe ages, the observer centered causal horizon $R_U(t)$ expands. New matter and galaxies become included in the causally connected domain, and the mass $M(t)$ enclosed inside $R_U(t)$ increases. Therefore, the compactness factor

$$\frac{R_S(t)}{R_U(t)} = \frac{2GM(t)}{c^2 R_U(t)} \tag{133}$$

can grow when the ratio $M(t)/R_U(t)$, or equivalently $R_S(t)/R_U(t)$, increases with time [6].

For an approximately homogeneous distribution at a given epoch,

$$M(t) = \frac{4\pi}{3} R_U(t)^3 \rho_m(t), \tag{134}$$

so that

$$\frac{R_S(t)}{R_U(t)} = \frac{8\pi G}{3c^2}\rho_m(t) R_U(t)^2. \tag{135}$$

This expression shows why a very low-density universe can still enter a high-compactness regime on sufficiently large causal scales. The relevant quantity is not the local matter density alone, but the horizon scale combination $\rho_m(t)R_U(t)^2$.

The total GSE dark energy density changes sign when

$$\frac{5\beta}{14}\frac{R_S(t)}{R_U(t)} - 1 = 0. \tag{136}$$

Equivalently,

$$R_U(t) = \frac{5\beta}{14}R_S(t). \tag{137}$$

Before this threshold is reached, $\rho_{\Lambda_m} < 0$. After it is crossed,

$$\rho_{\Lambda_m} > 0, \tag{138}$$

and the total GSE contribution becomes a positive dark energy density [6].

Positive dark energy density alone is not yet sufficient for accelerated expansion. Following the standard ΛCDM description of dark energy, in which $w_\Lambda = -1$ [23], we adopt the background-level approximation

$$w_{\Lambda_m} \simeq -1. \tag{139}$$

Under this assumption, accelerated expansion begins when

$$\rho_{\Lambda_m} > \frac{1}{2}\rho_m. \tag{140}$$

Using Eq. (131), this condition is equivalent to

$$R_U(t) < R_{\mathrm{crit,U}}(t), \tag{141}$$

where

$$R_{\mathrm{crit,U}}(t) \simeq 0.279\,\beta R_S(t). \tag{142}$$

Because $R_{\mathrm{crit,U}}(t)$ is proportional to $R_S(t)$, it moves outward when the enclosed causal mass $M(t)$ grows. Thus, even after a long decelerating era, the universe can enter a late accelerated phase once the growing causal compactness satisfies

$$\frac{R_S(t)}{R_U(t)} > \frac{7}{5\beta}\left(1 + \sqrt{\frac{17}{7}}\right) \simeq \frac{3.58}{\beta}. \tag{143}$$

For $\beta = 1.5$, this becomes

$$\frac{R_S(t)}{R_U(t)} > 2.39. \tag{144}$$

The resulting sequence is therefore

$$\begin{gathered}\text{early acceleration driven by total GSE (inflation)}\\ \longrightarrow \text{a decelerating phase during the radiation era and the matter era}\\ \longrightarrow \text{late-time dark energy acceleration.}\end{gathered} \tag{145}$$

In this picture, the late-time accelerated expansion does not come from an externally added cosmological constant. It arises when the total GSE of the growing causal domain becomes a sufficiently large positive dark energy density. The expansion of the causal horizon increases the enclosed gravitational source, raises the Schwarzschild equivalent radius, and eventually drives the system into the positive total GSE dark energy regime [6].

5.6 Cosmic History from Total GSE Dark Energy

The central result of this section is that the total GSE dark energy density of a causal cosmic domain describes cosmic expansion through

$$\rho_{\Lambda_m} = \frac{\beta \rho_m}{2} \frac{R_S}{R_U} \left(\frac{5\beta}{14} \frac{R_S}{R_U} - 1 \right). \tag{146}$$

Here $R_U(t)$ is the causal radius of the relevant cosmic domain, and $R_S(t) = 2GM(t)/c^2$ is the Schwarzschild equivalent radius generated by the matter sector mass $M(t)$, including baryonic matter and dark matter, contained inside that causal domain [6].

The factor

$$\left(\frac{5\beta}{14} \frac{R_S}{R_U} - 1 \right) \tag{147}$$

determines the sign of ρ_{Λ_m}. Thus,

$$\rho_{\Lambda_m} = 0 \quad \Longleftrightarrow \quad R_U = \frac{5\beta}{14} R_S = R_{\min,E}. \tag{148}$$

For $R_U < R_{\min,E}$, the total GSE density becomes positive and corresponds to a positive dark energy density. If this component has a background-level equation of state $w_\Lambda \simeq -1$, it carries negative pressure and can drive accelerated expansion when it becomes sufficiently large.

For $R_U > R_{\min,E}$, the total GSE density becomes negative. In that case, the corresponding pressure is positive for $w_\Lambda \simeq -1$, and the contribution acts in the direction of deceleration rather than accelerated expansion [6].

Positive ρ_{Λ_m} is not by itself sufficient for acceleration. In a radiation-dominated epoch, accelerated expansion begins when

$$\rho_{\Lambda_m} \gtrsim \rho_r. \tag{149}$$

In a matter-dominated epoch, where the matter pressure is negligible, the corresponding condition is

$$\rho_{\Lambda_m} > \frac{1}{2} \rho_m. \tag{150}$$

For the matter-dominated case, we write this condition as

$$R_U < R_{\text{crit,U}}, \qquad R_{\text{crit,U}} = \frac{5\beta}{7\left(1 + \sqrt{17/7}\right)} R_S \simeq 0.279\, \beta R_S. \tag{151}$$

The resulting cosmic history has three stages.

1) **Early total GSE accelerated expansion.** In the very early universe, the causal domain is extremely compact, and the total GSE dark energy density can become larger than the radiation density:

$$\rho_{\Lambda_m} > \rho_r. \tag{152}$$

This produces an early inflation-like accelerated expansion. The estimates in this section show that the total GSE mechanism can reach the characteristic time and energy density scales usually associated with the standard inflationary epoch [6, 18–20, 39].

2) **Decelerating expansion during the radiation era and the matter era.** As the early causal domain expands, the compactness factor weakens. The total GSE dark energy density falls below the radiation density, and the universe enters a decelerating radiation

era. After the radiation-to-matter transition, the matter-dominated era also remains decelerating as long as

$$\rho_{\Lambda_m} < \frac{1}{2}\rho_m. \tag{153}$$

When $\rho_{\Lambda_m} < 0$, the total GSE contribution is attractive in the acceleration equation and can support the formation and growth of galaxies and large-scale cosmic structures [6].

3) **Late-time total GSE dark energy acceleration.** At late times, the causal horizon continues to grow. As new matter and galaxies become included in the causally connected domain, the enclosed mass $M(t)$ increases, and the Schwarzschild equivalent radius $R_S(t)$ grows relative to $R_U(t)$. This growth drives the bracketed factor in Eq. (146) from negative to positive and eventually makes

$$\rho_{\Lambda_m} > \frac{1}{2}\rho_m. \tag{154}$$

The universe then enters the late-time accelerated expansion era [6].

The sequence can be summarized as

$$\begin{aligned} &\text{early acceleration driven by total GSE (inflation)} \\ &\longrightarrow \text{a decelerating phase during the radiation era and the matter era} \\ &\longrightarrow \text{late-time total GSE dark energy acceleration.} \end{aligned} \tag{155}$$

Therefore, cosmic expansion is not a fatal objection to Black Hole Cosmology. In the present framework, both the early inflation-like phase and the late-time accelerated phase arise from the same total GSE dark energy density, while the intermediate decelerating era appears when this contribution is too small or negative [6].

6 Accelerated Expansion as Evidence for Black Hole Cosmology

6.1 Total GSE Dark Energy Density and Friedmann Equations

In the preceding section, cosmic acceleration was described through the total GSE dark energy density associated with a causal cosmic domain. The relevant scale is not the physical radius of a finite isolated object, but the causal radius $R_U(t)$, which may be identified with the physical particle horizon scale, or more generally with the observer-centered causal horizon used to define the cosmic domain. The total GSE of the matter contained inside this causal domain defines the total GSE dark energy density [6].

The total GSE density derived in the MOC and total GSE formulation is identified with the dark energy density [6],

$$\rho_{\Lambda_m} = \rho_{m-gs} - \rho_{gs}, \tag{156}$$

where $\rho_{gs} > 0$ denotes the positive magnitude of the attractive GSE density contribution, so that this contribution enters as $-\rho_{gs}$, and $\rho_{m-gs} > 0$ denotes the positive matter–GSE interaction density contribution. In terms of the matter density ρ_m, the causal radius R_U, and the Schwarzschild equivalent radius $R_S = 2GM/c^2$, where M denotes the enclosed matter-sector mass, including baryonic matter and dark matter, and does not include an independent dark energy component, the result becomes

$$\rho_{\Lambda_m}(\rho_m, R_U) = \frac{\beta\rho_m}{2}\frac{R_S}{R_U}\left(\frac{5\beta}{14}\frac{R_S}{R_U} - 1\right). \tag{157}$$

Equivalently, using

$$M = \frac{4\pi}{3}\rho_m R_U^3, \qquad \frac{R_S}{R_U} = \frac{8\pi G}{3c^2}\rho_m R_U^2, \tag{158}$$

and defining

$$c_1 \equiv \frac{4\pi G}{3c^2}, \qquad c_2 \equiv \frac{20\pi G}{21c^2}, \tag{159}$$

the same dark energy density can be written compactly as [6]

$$\rho_{\Lambda_m}(\rho_m, R_U) = c_1\beta\rho_m^2 R_U^2\left(c_2\beta\rho_m R_U^2 - 1\right). \tag{160}$$

The total GSE dark energy density enters the Friedmann equation through the total effective cosmic density,

$$H^2 = \frac{8\pi G}{3}\left(\rho_m + \rho_{\Lambda_m}\right) - \frac{kc^2}{a^2}. \tag{161}$$

Substituting Eq. (157) gives

$$H^2 = \frac{8\pi G\rho_m}{3}\left[1 + \frac{\beta}{2}\frac{R_S}{R_U}\left(\frac{5\beta}{14}\frac{R_S}{R_U} - 1\right)\right] - \frac{kc^2}{a^2}. \tag{162}$$

Thus, the background expansion rate is controlled not only by the matter density ρ_m, but also by the causal compactness ratio R_S/R_U. In a convention where the curvature parameter already absorbs the factor c^2, the last term may be written as $-k/a^2$.

The corresponding acceleration equation is

$$\frac{\ddot{a}}{a} = -\frac{4\pi G}{3}\left[\rho_m + \rho_{\Lambda_m} + \frac{3P_{\Lambda_m}}{c^2}\right]. \tag{163}$$

Writing

$$P_{\Lambda_m} = w_{\Lambda_m}\rho_{\Lambda_m}c^2, \tag{164}$$

this becomes

$$\frac{\ddot{a}}{a} = -\frac{4\pi G}{3}\left[\rho_m + \left(1 + 3w_{\Lambda_m}\right)\rho_{\Lambda_m}\right]. \tag{165}$$

For the background dark energy approximation $w_{\Lambda_m} \simeq -1$ [15, 23], one obtains

$$\frac{\ddot{a}}{a} \simeq -\frac{4\pi G\rho_m}{3}\left[1 - \beta\frac{R_S}{R_U}\left(\frac{5\beta}{14}\frac{R_S}{R_U} - 1\right)\right]. \tag{166}$$

Equation (166) shows that the sign of cosmic acceleration is governed by the total GSE compactness factor. In a matter-dominated epoch, accelerated expansion begins when

$$\rho_{\Lambda_m} > \frac{1}{2}\rho_m, \tag{167}$$

or equivalently when

$$R_U < R_{\mathrm{crit,U}}, \qquad R_{\mathrm{crit,U}} \simeq 0.279\,\beta R_S. \tag{168}$$

Here β is the dimensionless structural coefficient of the GSE functional, determined by the effective matter distribution of the gravitating system. For a uniform Newtonian sphere, $\beta = 3/5$ [31], while in relativistic or compact astrophysical configurations it is naturally of order unity, typically in the range $\beta \sim 1$–2 [32–34]. After cosmic structure formation, the large-scale matter distribution evolves slowly enough that β may be treated as approximately constant in the late-time cosmological estimate [6].

Equation (157) shows that dark energy is not an independent component separated from matter. Instead, it is a matter-induced component generated by the total GSE of the matter sector [6]. Since R_S is itself determined by ρ_m and R_U, the **dark energy density is fixed by the matter density ρ_m and the causal radius R_U**, or equivalently by the causal compactness ratio R_S/R_U [6]. A low-density universe can therefore still generate a significant total GSE dark energy contribution when the causally connected region is sufficiently large.

6.2 Sign Transition and Accelerated Expansion

The factor $\left(\frac{5\beta}{14}\frac{R_S}{R_U}-1\right)$ determines the sign of the total GSE dark energy density [6]. The sign transition occurs when this factor vanishes:

$$R_U = \frac{5\beta}{14}R_S = R_{\mathrm{min},E}. \tag{169}$$

Here $R_{\mathrm{min},E}$ denotes the algebraic sign transition scale of the instantaneous cosmological compactness relation, not a fixed lower bound on the evolving causal radius.

For

$$R_U < \frac{5\beta}{14}R_S, \tag{170}$$

the total GSE dark energy density becomes positive:

$$\rho_{\Lambda_m} > 0. \tag{171}$$

For

$$R_U > \frac{5\beta}{14}R_S, \tag{172}$$

the total GSE dark energy density becomes negative:

$$\rho_{\Lambda_m} < 0. \tag{173}$$

Following the standard ΛCDM description of dark energy, in which $w_\Lambda = -1$ [15, 23], we adopt $w_{\Lambda_m} \simeq -1$ for the positive total GSE dark energy sector as a fiducial background approximation. This approximation is also consistent with the effective continuity relation: when the total GSE dark energy density varies slowly over a Hubble time, $|\dot{\rho}_{\Lambda_m}| \ll 3H\rho_{\Lambda_m}$, the corresponding effective equation of state parameter approaches $w_{\Lambda_m} \simeq -1$.

In the MOC simulation, this condition is realized approximately during the late-time acceleration epoch, where ρ_{Λ_m} evolves slowly near its broad maximum [6]. Under this approximation, a positive total GSE dark energy density carries negative pressure and can drive accelerated expansion when it becomes sufficiently large. In a matter-dominated epoch, the acceleration condition is

$$\rho_{\Lambda_m} > \frac{1}{2}\rho_m. \tag{174}$$

Using Eq. (157), we write this condition as

$$R_U < R_{\mathrm{crit,U}}, \tag{175}$$

where

$$R_{\mathrm{crit,U}} = \frac{5\beta}{7\left(1+\sqrt{17/7}\right)}R_S \simeq 0.279\,\beta R_S. \tag{176}$$

Thus, the sign transition of ρ_{Λ_m} occurs at $R_U = R_{\mathrm{min},E}$, while the onset of accelerated expansion occurs at the stronger condition $R_U < R_{\mathrm{crit,U}}$.

For the present observable universe, the causal radius is approximately $R_U \simeq 46.5\,\mathrm{Gly}$, while the matter-only Schwarzschild equivalent radius generated by baryonic matter and dark matter inside the particle horizon is $R_S \simeq 150.4\,\mathrm{Gly}$.

For the MOC baseline value $\beta \simeq 1.6$, based on the earlier CMB-based MOC estimate $\beta \simeq 1.6172$ [6], Eq. (176) gives

$$R_{\mathrm{crit,U}} \simeq 0.279(1.6)(150.4\,\mathrm{Gly}) \simeq 67.1\,\mathrm{Gly}. \tag{177}$$

Therefore, the present observable universe satisfies

$$R_U \simeq 46.5\,\mathrm{Gly} < R_{\mathrm{crit,U}} \simeq 67.1\,\mathrm{Gly}. \tag{178}$$

In the present framework, this places the current observable universe in the accelerated expansion regime.

This gives a direct link between the horizon growth mechanism discussed in Sec. 5 and late-time acceleration. As the causal horizon $R_U(t)$ expands, newly connected matter becomes included in the causal gravitational domain [12,15]. The enclosed matter mass $M(t)$ increases, and the compactness factor

$$\frac{R_S(t)}{R_U(t)} = \frac{2GM(t)}{c^2 R_U(t)} \tag{179}$$

can grow when the mass per causal radius, $M(t)/R_U(t)$, increases.

In a simple uniform density comparison at a fixed epoch,

$$M \propto R_U^3, \qquad R_S \propto R_U^3, \qquad \frac{R_S}{R_U} \propto R_U^2. \tag{180}$$

For the time-dependent cosmological case, the corresponding condition is that $\rho_m(t) R_U(t)^2$, or equivalently $R_S(t)/R_U(t)$, increases. Thus, even during a decelerating expansion era, the causal compactness can increase as the gravitationally connected region grows. Once $R_U(t)$ becomes smaller than $R_{\mathrm{crit,U}}(t)$, the total GSE dark energy density becomes large enough to drive late-time accelerated expansion [6].

6.3 Present Epoch Estimate and Cosmic History Consistency

For the present observable universe, we use the CMB-based background values

$$H_0 = 67.360\,\mathrm{km\,s^{-1}\,Mpc^{-1}}, \qquad \Omega_m = 0.3158, \tag{181}$$

together with the present critical density $\rho_c = 8.5227 \times 10^{-27}\,\mathrm{kg\,m^{-3}}$.

The corresponding present matter density, including baryonic matter and dark matter, is

$$\rho_{m,0} = \Omega_m \rho_c \simeq 2.69147 \times 10^{-27}\,\mathrm{kg\,m^{-3}}. \tag{182}$$

Using the present physical particle horizon radius

$$R_U(t_0) = R_{p,\mathrm{phys}}(t_0) = a_0 \chi_p(t_0) \simeq 46.114\,\mathrm{Gly}, \qquad a_0 = 1. \tag{183}$$

Elsewhere in this paper, the commonly quoted approximate value $R_U \simeq 46.5\,\mathrm{Gly}$ is used where an order of magnitude estimate is sufficient. In the present CMB-based calculation, we use $R_U(t_0) \simeq 46.114\,\mathrm{Gly}$, evaluated consistently from the adopted background parameters [6,15].

The matter-sector mass enclosed inside the particle horizon is

$$M(t_0) = \frac{4\pi}{3} \rho_{m,0} R_U(t_0)^3 \simeq 9.3616 \times 10^{53}\,\mathrm{kg}. \tag{184}$$

The corresponding matter-only Schwarzschild equivalent radius is

$$R_S(t_0) = \frac{2GM(t_0)}{c^2} \simeq 146.967\,\text{Gly}. \tag{185}$$

Therefore,

$$\frac{R_S(t_0)}{R_U(t_0)} \simeq \frac{146.967}{46.114} \simeq 3.187. \tag{186}$$

Using the CMB-based MOC structural coefficient $\beta = 1.6172$, Eq. (157) gives

$$\begin{aligned}\rho_{\Lambda_m}(t_0) &= \frac{1.6172\,\rho_{m,0}}{2}\left(\frac{146.967}{46.114}\right)\left[\frac{5(1.6172)}{14}\left(\frac{146.967}{46.114}\right) - 1\right] \\ &\simeq 5.8314 \times 10^{-27}\,\text{kg}\,\text{m}^{-3} \\ &\simeq 0.6842\,\rho_c. \end{aligned}\tag{187}$$

This value is consistent with the observed magnitude of the present dark energy density. The agreement supports the interpretation that the **observed dark energy density can be identified with the total GSE of the matter sector** inside the causal domain [6].

The quantities entering Eq. (157) and (160) do not play the role of arbitrary cosmological fitting parameters. The coefficient β is the structural integration coefficient of the GSE functional; it equals $3/5$ for a uniform Newtonian sphere and takes values of order unity, typically in the range $1 \lesssim \beta \lesssim 2$, in relativistic high-compactness configurations [31–34]. The radius R_U is fixed by the particle horizon scale, and R_S is fixed by the matter mass contained inside that horizon.

Therefore, the total GSE dark energy density explains the observed dark energy density using the GSE structure already present in existing gravitational theory, with limited phenomenological freedom once the matter density, causal radius, and structural coefficient are specified [6].

In this sense, the total GSE expression has a simplicity comparable to the cosmological constant, but with a physical origin. Instead of introducing a constant vacuum energy density as an independent input, the present framework relates the observed dark energy density to the total GSE of the matter content inside the causal horizon.

The present epoch estimate can also be compared with the time evolution of the same total GSE dark energy density. As a complementary consistency test, Fig. 4 and Table 2 show a CMB-based cosmic history simulation using the same functional form for $\rho_{\Lambda_m}(t)$. The simulation uses the standard matter abundance, $\Omega_m \simeq 0.3158$, and a constant structure coefficient $\beta = 1.6172$. This simulation shows that, with the structural coefficient β held fixed rather than treated as an adjustable fitting parameter, the total GSE density function still reproduces the qualitative sequence associated with the observed cosmic history: an early negative total GSE contribution that supports deceleration and large-scale cosmic structure formation, a sign transition, the onset of accelerated expansion, and a slowly varying positive dark energy density near the present epoch [6, 15].

For clarity, Fig. 4 and Table 2 adopt the time-dependent cosmological prescription developed in the MOC framework [6]. In this prescription, the comoving particle horizon $\chi_p(t)$ is used as the causal interaction scale of the total GSE, whereas $R_{\text{phys}}(t) = a(t)\chi_p(t)$ determines the physical volume and the enclosed matter mass, $M(t) = (4\pi/3)\rho_m(t)R^3_{\text{phys}}(t)$. The GSE interaction terms are therefore evaluated using $\chi_p(t)$, while the corresponding physical densities are obtained using the physical volume $V_{\text{phys}}(t) = (4\pi/3)R^3_{\text{phys}}(t)$. At the present epoch, $a_0 = 1$, so that $\chi_p(t_0) = R_{\text{phys}}(t_0) = R_U(t_0)$, and this prescription reduces to the present-epoch expression used above. The full cosmological derivation and analysis are given in Ref. [6].

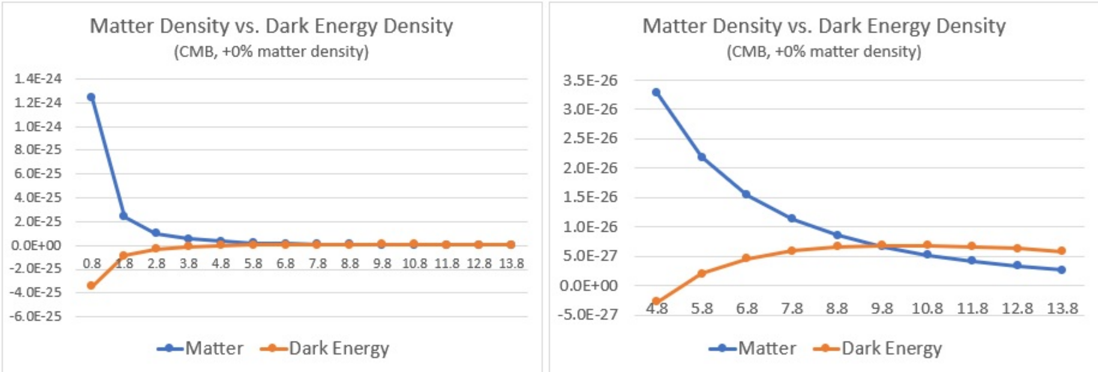

Figure 4: **Matter density and total GSE dark energy density in a CMB-based cosmic history simulation.** The simulation uses the standard matter abundance, $\Omega_m \simeq 0.3158$, with no matter enhancement and a constant structure coefficient $\beta = 1.6172$. The total GSE dark energy density is negative for $t \lesssim 5.38\,\text{Gyr}$, supporting deceleration and large-scale cosmic structure formation. It becomes positive after the sign transition and satisfies the acceleration condition near $t \simeq 7.72\,\text{Gyr}$. The dark energy density reaches a broad maximum over $t \simeq 9.8$–$10.8\,\text{Gyr}$ and then decreases slowly toward the present epoch.

Age (Gyr)	Scale $a(t)$	Constant β	Comoving Horizon $\chi_p(t)$ (Gly)	Physical Horizon $R_{\text{phys}}(t)$ (Gly)	**Matter** $\rho_m(t)$	Repulsive $\rho_{m\text{-}gs}(t)$	Attractive $-\rho_{gs}(t)$	**Dark Energy** $\rho_{\Lambda_m}(t)$
					$(10^{-27}\,\text{kg}\,\text{m}^{-3})$			
0.8	0.1295	1.6172	17.763	2.300	1239.310	129.425	-473.872	**-344.447**
1.8	0.2226	1.6172	23.521	5.236	244.013	78.345	-163.596	**-85.252**
2.8	0.2998	1.6172	27.369	8.205	99.884	58.790	-90.669	**-31.879**
3.8	0.3694	1.6172	30.368	11.218	53.395	47.636	-59.673	**-12.037**
4.8	0.4346	1.6172	32.862	14.282	32.788	40.111	-42.910	**-2.798**
5.8	0.4972	1.6172	35.013	17.408	21.898	34.521	-32.531	**1.990**
6.8	0.5584	1.6172	36.912	20.612	15.458	30.102	-25.523	**4.579**
7.8	0.6190	1.6172	38.614	23.902	11.348	26.465	-20.505	**5.960**
8.8	0.6796	1.6172	40.156	27.290	8.575	23.389	-16.756	**6.632**
9.8	0.7408	1.6172	41.567	30.793	6.620	20.733	-13.862	**6.870**
10.8	0.8031	1.6172	42.864	34.424	5.196	18.400	-11.569	**6.831**
11.8	0.8668	1.6172	44.064	38.195	4.133	16.343	-9.724	**6.619**
12.8	0.9323	1.6172	45.178	42.119	3.321	14.515	-8.215	**6.299**
13.8	1.0000	1.6172	46.114	46.114	2.691	12.766	-6.935	**5.831**

Table 2: **CMB-based cosmic history simulation of the total GSE dark energy density.** The simulation assumes the standard matter abundance, $\Omega_m \simeq 0.3158$ and a constant structure coefficient $\beta = 1.6172$. **The total GSE dark energy density is negative for** $t \lesssim 5.38\,\text{Gyr}$, changes sign near $t \simeq 5.38\,\text{Gyr}$, and satisfies the acceleration condition $\rho_{\Lambda_m} > \rho_m/2$ near $t \simeq 7.72\,\text{Gyr}$. It reaches a broad maximum over $t \simeq 9.8$–$10.8\,\text{Gyr}$ and then decreases slowly toward the present epoch. At $t_0 \simeq 13.8\,\text{Gyr}$, the model gives $\rho_{\Lambda_m}(t_0) \simeq 5.831 \times 10^{-27}\,\text{kg}\,\text{m}^{-3}$, consistent with $\rho_{\Lambda_m} \simeq 0.684\rho_c$. **This single $\rho_{\Lambda_m}(t)$ equation provides a unified account of (i) enhanced early structure growth, including the rapid assembly of massive galaxies reported by JWST [40, 41], (ii) the transition to accelerated expansion ~ 5 Gyr ago, (iii) the present value of the dark energy density, (iv) late-time quasi-constant dark energy density, and (v) hints of weakening dark energy [16].**

The simulation provides a time-dependent version of the single epoch estimate in Eq. (187). During the early and intermediate cosmic epochs, ρ_{Λ_m} is negative or too small to dominate the matter component, so the universe remains in a decelerating phase and large-scale cosmic structures can grow. As the causal horizon expands, the enclosed matter mass increases, and the compactness factor $\frac{R_S(t)}{R_U(t)} = \frac{2GM(t)}{c^2 R_U(t)}$ grows when the mass per causal radius, $M(t)/R_U(t)$, increases. This drives the total GSE density through a sign transition and eventually into the regime $\rho_{\Lambda_m} > \rho_m/2$, where late-time accelerated expansion begins.

This result strengthens the interpretation proposed in this paper. The model does not merely reproduce the present epoch dark energy density; the same total GSE density function also yields a plausible cosmic sequence consisting of structure-forming deceleration, a transition to positive dark energy, the onset of late-time acceleration, and a slowly evolving positive dark energy density near the present epoch [6].

6.4 Meaning for Black Hole Cosmology

The total GSE density function changes the role of cosmic acceleration in Black Hole Cosmology. The historical objection treated the expansion of the universe as evidence against the idea that the universe is related to a black hole configuration [5]. In the present framework, the same causal compactness that places the observable universe inside its own Schwarzschild equivalent radius also generates the dark energy density responsible for accelerated expansion.

Thus, accelerated expansion is not an external addition to Black Hole Cosmology. It arises from the total GSE of the large-scale matter distribution inside the causal horizon. The present epoch value $\rho_{\Lambda_m} \simeq 0.685\rho_c$ provides a quantitative bridge between the causal compactness condition, the total GSE dark energy density function, and the accelerated expansion of the universe [6].

For the present observable universe, the matter content inside the particle horizon gives

$$R_S \simeq 150.4\,\text{Gly}, \qquad R_U \simeq 46.5\,\text{Gly}. \tag{188}$$

Therefore,

$$\frac{R_S}{R_U} \simeq \frac{150.4}{46.5} \simeq 3.23 > 1. \tag{189}$$

In this compactness sense, the observable universe lies inside the Schwarzschild equivalent horizon scale generated by its own matter content. Therefore, the incompleteness of classical theory inside black hole interiors limits any attempt to explain cosmic acceleration solely within unmodified classical GR.

This result also gives a sharper interpretation of the limitation of classical General Relativity. Classical GR predicts a singularity at the endpoint of black hole collapse, and this singularity prediction signals that the unmodified classical theory is not a complete description of black hole interiors [11, 17]. **If General Relativity is incomplete inside a black hole, then it is also incomplete in the observable universe.**

In this view, dark energy is not merely an unexplained extra component added to cosmology. It is the observational form taken by the missing gravitational principle required in a black hole interior compactness regime. Equivalently, we interpret the accelerated expansion of the universe and the existence of dark energy as evidence that the unmodified classical GR description is incomplete at the cosmological scale, just as it is incomplete in the deep interior of a black hole.

The central conclusion of this section is therefore direct. The total GSE density function turns the main objection to Black Hole Cosmology into a testable prediction.

Depending on the compactness ratio, the total GSE dark energy density can be either negative or positive. The sign transition occurs at $R_U = R_{\min,E}$, while accelerated expansion requires the stronger condition $R_U < R_{\text{crit,U}}$. Thus, even inside a cosmological black hole domain satisfying $R_U < R_S$, decelerating expansion can occur when $R_U > R_{\min,E}$ or when the positive total GSE dark energy density is still below the acceleration threshold.

For the present observable universe, using the commonly quoted approximate causal radius $R_U \simeq 46.5\,\text{Gly}$, the matter-sector mass inside the causal domain gives the corresponding matter-only Schwarzschild equivalent radius $R_S \simeq 150.4\,\text{Gly}$. For the associated present-epoch estimate, we use $\beta = 1.595$. The acceleration threshold is then

$$R_{\text{crit,U}} \simeq 0.279\beta R_S \simeq 0.279(1.595)(150.4\,\text{Gly}) \simeq 67.0\,\text{Gly}. \tag{190}$$

Since the present observable causal radius satisfies

$$R_U \simeq 46.5\,\text{Gly} < R_{\text{crit,U}} \simeq 67.0\,\text{Gly}, \tag{191}$$

the observable universe lies in the accelerated expansion regime within the present framework. Consequently, accelerated expansion is not a contradiction to Black Hole Cosmology. Rather, it arises because the observable universe lies sufficiently deep inside its Schwarzschild equivalent horizon that the total GSE dark energy sector becomes large enough to drive cosmic acceleration. In this sense, **accelerated expansion is transformed from an objection against Black Hole Cosmology into strong evidence for it.**

6.5 Closed Black Hole Universes and Cosmological Black Holes

Total GSE dynamics gives two distinct versions of the black hole cosmology idea. The first is a closed black hole universe formed by a finite collapsing matter distribution. The second is the cosmological black hole relevant to our observable universe. These two cases share the same total GSE finite-radius principle, but they differ in their global setting.

6.5.1 Closed Black Hole Universes

The first case is a closed black hole universe formed by a finite collapsing matter distribution. If a sufficiently large and finite matter distribution contracts and forms a black hole, the resulting object can become an isolated, closed black hole. In the total GSE description, the interior does not proceed toward a point singularity. Instead, the total GSE energy landscape contains finite characteristic radii, including the stable equilibrium radius

$$R_{gs} = \frac{5\beta}{7} R_S, \tag{192}$$

and the energy-limited radii [7]. For a sufficiently massive black hole, these characteristic radii are macroscopic. A large closed black hole universe can therefore contain an extended interior domain with weak local curvature and approximately flat geometry. In principle, such an interior can be large enough to contain galaxies, stars, planets, and intelligent life [7].

- **Macroscopic equilibrium scale and density benchmark.**

  A simple order of magnitude estimate illustrates the macroscopic character of the finite-radius interior. Instead of using the average density inside the Schwarzschild horizon, consider the average density inside the stable equilibrium radius R_{gs}:

  $$\bar{\rho}_{gs} = \frac{3M}{4\pi R_{gs}^3}. \tag{193}$$

Using
$$R_{gs} = \frac{5\beta}{7} R_S = \frac{10\beta GM}{7c^2}, \tag{194}$$
the average density becomes
$$\bar{\rho}_{gs} = \frac{3c^6}{32\pi G^3 M^2} \left(\frac{7}{5\beta} \right)^3. \tag{195}$$
Thus, the average density inside R_{gs} decreases as
$$\bar{\rho}_{gs} \propto M^{-2}. \tag{196}$$
As the total mass increases, the characteristic interior radius grows linearly with M, while the average density decreases quadratically.

As a representative macroscopic density scale compatible with ordinary complex matter, consider the density of water,
$$\rho_w \simeq 10^3 \,\mathrm{kg\,m^{-3}}. \tag{197}$$
The condition
$$\bar{\rho}_{gs} = \rho_w \tag{198}$$
gives
$$M_w = \left[\frac{3c^6}{32\pi G^3 \rho_w} \left(\frac{7}{5\beta} \right)^3 \right]^{1/2} \simeq 2.25 \times 10^8 \,\beta^{-3/2} M_\odot. \tag{199}$$
For the fiducial interior estimate, one may take $\beta = 1$, for which $R_{gs} < R_S$. This gives
$$M_w \simeq 2.25 \times 10^8 M_\odot, \qquad R_S \simeq 4.44\,\mathrm{AU}, \qquad R_{gs} \simeq 3.17\,\mathrm{AU}. \tag{200}$$
Thus, for sufficiently massive black holes, the characteristic total GSE radii are macroscopic rather than microscopic.

- **Stable equilibrium and the total GSE radial response.**

  At $R = R_{gs}$, the attractive GSE term and the repulsive matter–GSE interaction term cancel exactly:
  $$D_T U(R_{gs}) = 0. \tag{201}$$
  Therefore, R_{gs} is not characterized by a large net inward gravitational acceleration. It is a stable equilibrium radius at which the two contributions to the total GSE radial response balance each other. In sufficiently massive systems, local curvature and tidal gradients can remain weak over extended interior regions.

- **Tidal environment near the stable equilibrium radius.**

  The tidal environment at this mass scale is weak over human-scale and spacecraft-scale lengths. As a conservative benchmark, the radial tidal differential acceleration in a freely falling Schwarzschild frame may be estimated as
  $$\Delta a_{\mathrm{Schw}} \simeq \frac{2GM}{R_{gs}^3} L. \tag{202}$$
  For $M = M_w \simeq 2.25 \times 10^8 M_\odot$, $\beta = 1$, and a characteristic length $L = 2\,\mathrm{m}$, this gives
  $$\Delta a_{\mathrm{Schw}}(R_{gs}) \simeq 1.12 \times 10^{-6} \,\mathrm{m\,s^{-2}}, \tag{203}$$

which is approximately 1.14×10^{-7} times the gravitational acceleration at the Earth's surface. The differential acceleration across a human-scale body is therefore far below the level required for tidal disruption.

The total GSE radial response gives a consistent effective gradient estimate near the stable equilibrium radius. Linearizing $D_T U(R)$ around $R = R_{gs}$ gives

$$D_T U(R) \simeq -\frac{\beta GM}{R_{gs}^3}\left(R - R_{gs}\right). \tag{204}$$

The corresponding effective differential radial acceleration over a length L is

$$\Delta a_{\mathrm{GSE}} \sim \frac{\beta GM}{R_{gs}^3} L. \tag{205}$$

For the same fiducial parameters and $L = 2\,\mathrm{m}$,

$$\Delta a_{\mathrm{GSE}} \sim 5.59 \times 10^{-7}\,\mathrm{m\,s^{-2}}. \tag{206}$$

This value is likewise extremely small. It represents an effective gradient of the collective total GSE radial dynamics rather than a complete local tidal tensor. A rigorous local tidal analysis requires an interior metric consistent with total GSE dynamics and the corresponding geodesic-deviation equation.

- **Implications for survivability and habitability.**

  The density and tidal estimates do not by themselves guarantee habitability, since temperature, radiation, chemical history, matter distribution, and structure formation must also be considered. They do show, however, that **a sufficiently massive closed black hole can possess a macroscopic nonsingular interior whose average density and tidal environment are not intrinsically hostile to complex life.**

  These results also lead to an additional physically interesting possibility. For a sufficiently massive black hole, an infalling human or spacecraft may survive the tidal environment and reach the macroscopic nonsingular core region without undergoing tidal disruption. In particular, for black holes with masses of order $10^8 M_\odot$ or larger, the tidal gradients near R_{gs} are sufficiently weak on human and spacecraft length scales. Whether controlled arrival or long-term survival is possible depends additionally on the interior geometry, thermal and radiative environment, matter distribution, and the mechanism through which the infalling object loses its radial velocity. Nevertheless, within the total GSE framework, survival of the infall to the finite-radius core is not excluded by tidal forces.

6.5.2 The Observable Universe as a Cosmological Black Hole

The second case is the one relevant to our observable universe. In this case, the claim is not that the entire universe is an isolated Schwarzschild black hole surrounded by an exterior vacuum. The large-scale universe may contain matter and energy distributed nearly uniformly over a region much larger than the present observable universe. Our observable universe is then described as an observer-centered causal domain inside a much larger cosmological matter distribution [6].

For a spherical causal domain centered on an observer, the relevant gravitational content is the quasi-local matter-sector mass contained inside the physical particle horizon, or more generally inside the observer-centered causal horizon [12, 15]. As established in Sec. 2.3, the use of $R_S(t) = 2GM(t)/c^2$ in the present cosmological setting is a spherical-domain quasi-local compactness diagnostic within the FLRW background. It does not replace the FLRW metric with a Schwarzschild vacuum metric. By the usual shell theorem intuition and by the cosmological application of Birkhoff's theorem, **the acceleration of a spherical domain in a homogeneous fluid universe is determined by the fluid enclosed within that domain** [8, 12, 35]. Accordingly, the corresponding Schwarzschild-equivalent radius may be written as $R_S(t) = \frac{2GM(t)}{c^2}$, where $M(t)$ denotes the enclosed matter-sector mass, including baryonic matter and dark matter, and does not include an independent dark energy component [6].

For the present observable universe, the matter-only Schwarzschild equivalent horizon scale is approximately $R_S \simeq 150.4\,\text{Gly}$, whereas the observable universe causal radius is approximately $R_U \simeq 46.5\,\text{Gly}$.

Thus,

$$\frac{R_S}{R_U} \simeq 3.23 > 1. \tag{207}$$

If the same observable volume is evaluated using the standard critical density ρ_c as a comparison scale, the corresponding Schwarzschild equivalent horizon scale becomes approximately

$$R_{S,c} \simeq 477\,\text{Gly}, \tag{208}$$

giving

$$\frac{R_{S,c}}{R_U} \sim \frac{477\,\text{Gly}}{46.5\,\text{Gly}} \sim 10. \tag{209}$$

Therefore, the conclusion $R_S/R_U > 1$ is not a marginal result of the matter-only estimate; it becomes even stronger when the critical density scale is used [6, 7].

In this compactness sense, the present observable universe lies inside its own Schwarzschild equivalent horizon scale. This does not require the whole universe to be a finite isolated Schwarzschild black hole. It means that our observable universe is a high-compactness causal domain inside a much larger nearly homogeneous cosmic matter distribution.

This interpretation also explains why the black hole compactness condition can persist as the universe evolves. As the causal horizon expands, new matter and galaxies become included in the gravitationally connected region. The enclosed matter-sector mass $M(t)$ then increases, and the corresponding Schwarzschild equivalent horizon scale grows as $R_S(t) = \frac{2GM(t)}{c^2}$.

In a simple uniform density comparison at a fixed epoch,

$$M \propto R_U^3, \qquad R_S \propto R_U^3, \qquad \frac{R_S}{R_U} \propto R_U^2. \tag{210}$$

For the time-dependent cosmological case, the corresponding condition is that $\rho_m(t)R_U(t)^2$, or equivalently $R_S(t)/R_U(t)$, increases. Thus, even during a decelerating expansion era, the causal compactness can increase as the gravitationally connected region grows. If the supply of newly connected matter later becomes asymptotically limited, the enclosed matter-sector mass $M(t)$, and hence $R_S(t)$, may approach a finite asymptotic value. Even in that case, the Schwarzschild equivalent horizon scale generated by the enclosed matter can remain much larger than the causal radius.

In the present framework, even the inflationary phase is driven by the negative pressure associated with the total GSE dark energy density [6]. Therefore, within this model, the observable universe causal domain has remained inside the Schwarzschild-equivalent event horizon generated by the matter and radiation content enclosed within that domain from the inflationary epoch to the present.

6.5.3 The Time-Direction Problem in a Cosmological Black Hole

The apparent difference in the temporal placement of the singularity does not by itself constitute an independent objection to Black Hole Cosmology. In stellar collapse, matter enters from the exterior and, in the classical description, continues toward a decreasing areal radius after crossing the horizon. The singular boundary is therefore placed in the future of the infalling matter [11]. However, the appearance of this singular boundary signals the breakdown of the classical description rather than the existence of a physically established endpoint.

The absence of a physical singularity requires the continued inward evolution toward $R = 0$ to be interrupted. If the net radial response remained attractive at every smaller radius, no dynamical mechanism would prevent the contraction from proceeding toward the singular limit. A momentary cancellation of the inward acceleration at a single radius would not by itself provide a stable prevention of further collapse. On the inner side of the cancellation radius, the net radial response must reverse sign, producing a regime in which the repulsive response dominates over the attractive response and the radial acceleration is directed outward. Thus, the dynamical removal of the singular endpoint implies the existence of an inner repulsion-dominated branch and, consequently, a region in which outward radial motion is possible within the black hole interior.

Total GSE dynamics provides precisely this attractive-to-repulsive transition. In its cosmological application, when $R_U < R_{\mathrm{crit,U}}$, the positive total GSE density $\rho_{\Lambda m}$ is associated with negative effective pressure and drives accelerated expansion, while the same causal domain can simultaneously satisfy the black-hole-interior compactness condition $R_U < R_S$ [6]. Thus, outward cosmological evolution is compatible with black-hole-interior compactness. The conventional placement of the stellar-black-hole singularity in the future and the Big Bang singularity in the past therefore does not represent a physical contradiction. These different temporal placements reflect the opposite directions of classical evolution in stellar collapse and cosmology. Once the singular description is replaced by total GSE dynamics containing both attractive and repulsive branches, both inward and outward radial evolution can occur within a black-hole-compact configuration.

6.5.4 Possibility of Escape from a Cosmological Black Hole

The preceding discussion raises a natural question: is the observable universe causal domain merely similar to a black hole, or should it be regarded as a cosmological black hole? In the present framework, the decisive criterion is not whether the exterior region is an exact vacuum Schwarzschild spacetime. For a cosmological matter distribution, the more relevant question is whether the observer-centered causal domain can ever escape from the Schwarzschild equivalent event horizon generated by its own enclosed matter-sector mass. The escape condition would be

$$R_U(t) \geq R_S(t). \tag{211}$$

If this condition is never reached, the causal domain remains gravitationally confined in the quasi-local black hole sense.

The characteristic radii $R_{\mathrm{crit,U}}$ and $R_{\min,E}$ are both located well inside R_S. For $\beta \simeq 1.6$, one has $R_{\mathrm{crit,U}} \simeq 0.446 R_S$ and $R_{\min,E} \simeq 0.571 R_S$. Therefore, the transition from accelerated expansion to decelerating expansion occurs deep inside the Schwarzschild equivalent horizon scale. This structure gives the total GSE dynamics a restoring character: when the causal domain lies below the acceleration threshold, the positive total GSE dark energy density supports accelerated expansion, whereas once the domain passes beyond $R_{\min,E}$, the total GSE dark energy density becomes negative and contributes to deceleration.

This feedback suggests that the causal domain of radius R_U may not freely cross out of the cosmological black hole domain defined by the Schwarzschild equivalent scale R_S. Rather, it may evolve around the black hole interior characteristic scales set by $R_{\mathrm{crit,U}}$ and $R_{\min,E}$. This interpretation is also consistent with the observed sequence of cosmic expansion: an early accelerated inflationary phase, a subsequent decelerating expansion era, and a late-time accelerated expansion phase [13–15]. In the present framework, this sequence can be interpreted as phenomenological support for an oscillatory or evolution regulated by thresholds around the characteristic scales set by $R_{\mathrm{crit,U}}$ and $R_{\min,E}$ [6].

To clarify how this picture affects the possible escape of the causal domain, we now examine several concrete limiting cases.

Consider first the limiting case in which the enclosed matter-sector mass remains fixed after the present epoch. The present matter content gives

$$R_U \simeq 46.5\,\mathrm{Gly}, \qquad R_S \simeq 150.4\,\mathrm{Gly}. \tag{212}$$

If M remains fixed, then R_S also remains fixed. In that case, the causal radius crosses the acceleration threshold before it can reach the Schwarzschild equivalent event horizon. For $\beta \simeq 1.6$,

$$R_{\mathrm{crit,U}} \simeq 0.279\,\beta R_S \simeq 67.1\,\mathrm{Gly}, \tag{213}$$

while the sign transition of the total GSE dark energy density occurs at

$$R_{\min,E} = \frac{5\beta}{14} R_S \simeq 85.9\,\mathrm{Gly}. \tag{214}$$

This gives the ordering

$$R_U \simeq 46.5\,\mathrm{Gly} \longrightarrow R_{\mathrm{crit,U}} \simeq 67.1\,\mathrm{Gly} \longrightarrow R_{\min,E} \simeq 85.9\,\mathrm{Gly} \longrightarrow R_S \simeq 150.4\,\mathrm{Gly}. \tag{215}$$

Both characteristic radii, $R_{\mathrm{crit,U}}$ and $R_{\min,E}$, are still well inside $R_S \simeq 150.4\,\mathrm{Gly}$. The ordering in Eq. (215) therefore shows that the acceleration condition is lost well before the causal domain reaches $R_U = R_S$. It also shows that the total GSE dark energy density becomes negative throughout the interval

$$R_{\min,E} < R_U < R_S. \tag{216}$$

In this interval, both the matter contribution and the negative total GSE dark energy contribution act in the direction of deceleration in the acceleration equation [7].

This result, however, does not by itself prove that the causal domain must turn around before reaching $R_U = R_S$. The causal scale still retains an outward expansion velocity inherited from the earlier accelerated and decelerating phases. Therefore, a strict no-escape conclusion requires a time-dependent calculation of $R_U(t)$, $M(t)$, $\rho_{\Lambda_m}(t)$, and the expansion rate $H(t)$, including the velocity of the causal scale when $R_U(t)$ crosses $R_{\min,E}(t)$. The fixed mass estimate establishes a weaker but important result: before the causal domain can approach the Schwarzschild equivalent event horizon, total GSE dynamics first removes the acceleration contribution and then turns the total GSE dark energy contribution into a decelerating contribution [7].

The conclusion becomes more favorable to confinement if the causal horizon continues to grow and newly connected matter becomes included in the observable universe domain. In a simple uniform density comparison at a fixed epoch,

$$M \propto R_U^3, \qquad R_S \propto R_U^3, \qquad \frac{R_S}{R_U} \propto R_U^2. \tag{217}$$

For the time-dependent cosmological case, the corresponding condition is that $\rho_m(t)R_U(t)^2$, or equivalently $R_S(t)/R_U(t)$, increases. If this condition holds, the observable universe moves deeper into the high-compactness regime rather than escaping from it. In that case, the escape condition $R_U(t) \geq R_S(t)$ is pushed farther away.

A more subtle case may occur if the particle horizon later approaches a saturation scale and no further matter becomes included in the causal domain. In that case, the compactness ratio $R_S(t)/R_U(t)$ may decrease, and the causal domain may move toward the escape condition. However, the cosmological case is not equivalent to motion on the static total GSE potential of an isolated closed black hole. For an isolated finite collapse, the radial motion follows the gradient of $U_{gs-T}(R)$, and the total energy condition can determine whether the system remains bound or escapes [7]. In the cosmological case, the total GSE contribution enters the acceleration equation through the density $\rho_{\Lambda_m}(t)$ and its pressure contribution [6].

For this reason, the interval $R_{\mathrm{min},E} < R_U < R_{gs}$, which would belong to the outward-accelerating side of the static radial potential in an isolated closed black hole problem, cannot be transferred directly to the cosmological case. In the cosmological case, once $R_U > R_{\mathrm{min},E}$, the total GSE dark energy density is negative and therefore contributes to deceleration in the acceleration equation [6].

If the compactness decreases after horizon saturation, the causal domain must pass through the sign transition regime before it can reach $R_U(t) = R_S(t)$:

$$R_U(t) > R_{\mathrm{min},E}(t), \qquad \rho_{\Lambda_m}(t) < 0. \tag{218}$$

For $R_U > R_{\mathrm{min},E}$, the total GSE dark energy density contributes to deceleration throughout the remaining interval up to $R_U = R_S$. This makes escape dynamically disfavored in the present framework, but it does not constitute a strict no-escape theorem. A definitive conclusion requires solving the full time-dependent cosmological evolution.

For this reason, the present paper uses the term cosmological black hole in a quasi-local and dynamical sense. This term does not mean an isolated vacuum Schwarzschild black hole. It denotes a matter-filled, observer-centered causal domain satisfying

$$R_U(t) < R_S(t), \tag{219}$$

where $R_S(t)$ is the Schwarzschild-equivalent event horizon radius generated by the matter-sector mass enclosed within the causal domain.

The observable universe exhibits characteristics of a black hole interior not only in terms of compactness. Within total GSE dynamics, a repulsive gravitational response can arise inside the black hole interior, with the radial response becoming outward when

$$R < R_{gs} = \frac{5\beta}{7} R_S. \tag{220}$$

Moreover, the total GSE dark energy density becomes positive in a still deeper high-compactness region,

$$R < R_{\mathrm{min},E} = \frac{5\beta}{14} R_S, \qquad \rho_{\Lambda_m} > 0. \tag{221}$$

Thus, the observable universe reproduces not only the compactness condition $R_U < R_S$, but also the gravitational behavior that total GSE dynamics associates with the region inside the Schwarzschild-equivalent radius.

According to the present model, **the observable universe has remained in the regime $R_U(t) < R_S(t)$ from the inflationary epoch to the present.** It therefore satisfies the black hole interior compactness condition throughout its known cosmic evolution, while also exhibiting the total GSE dark energy and repulsive gravitational effects characteristic of this high-compactness regime. For these reasons, the observable universe is interpreted not merely as being analogous to a black hole, but as existing in a cosmological black hole state.

Whether this cosmological black hole domain remains permanently confined in the future depends on the time evolution of $R_U(t)$, $M(t)$, and $R_S(t)/R_U(t)$. The present analysis shows that total GSE dynamics removes the acceleration support before the causal domain reaches $R_U = R_S$, and that the total GSE dark energy density becomes negative over the interval $R_{\min,E} < R_U < R_S$. This indicates a transition into a decelerating-expansion regime before the Schwarzschild-equivalent radius is reached. Moreover, the observed cosmic sequence consists of early accelerated expansion during inflation, a subsequent decelerating era, late-time accelerated expansion, and recent indications of a weakening dark energy contribution. This sequence suggests a threshold-regulated, quasi-oscillatory evolution around $R_{\mathrm{crit,U}}$ [6]. Taken together, these features indicate that escape from the cosmological Schwarzschild-equivalent horizon is dynamically disfavored. However, a strict no-escape result cannot be concluded from this qualitative ordering alone and must be treated as a separate time-dependent problem.

6.6 Implication for the Black Hole Information Problem

The existence of a macroscopic nonsingular interior also has an important implication for the black hole information problem. In the conventional singular picture, information carried by infalling matter appears to be driven toward a zero volume singularity, while the exterior observer sees thermal Hawking radiation. This creates the well known tension between black hole evaporation and unitary quantum evolution [43–46].

A class of proposed resolutions places the relevant new physics near the Planck scale. In such pictures, the singularity may be avoided by replacing it with a Planck-scale core or remnant. Although this removes the classical singularity, it raises a severe storage problem: the information associated with a macroscopic black hole must somehow be encoded in an extremely small region [43, 45, 46].

The total GSE dynamics changes this aspect of the problem. The endpoint of collapse is not a Planck-scale remnant or a point singularity, but a finite-radius core characterized by the stable total GSE radius [7]. In particular,

$$R_{gs} = \frac{5\beta}{7} R_S. \tag{222}$$

For $0 < \beta < 7/5$, this radius lies inside the Schwarzschild radius. For $\beta = O(1)$, and in particular for the fiducial interior value $\beta \simeq 1$, it is a finite macroscopic fraction of R_S. Therefore, the primary interior information reservoir scales macroscopically with the black hole size:

$$V_{\mathrm{core}} \sim \frac{4\pi}{3} R_{gs}^3, \qquad R_{\mathrm{core}} \sim R_{gs} = O(R_S). \tag{223}$$

Thus, the information carried by the collapsing matter is not forced into a zero volume singularity or an extremely small Planck-scale remnant. It can remain associated with a large matter-filled nonsingular interior [7].

More precisely, in the total GSE picture, the stable matter core settles near R_{gs}, where the radial response of the total GSE dynamics vanishes [7]. During the relaxation from the horizon scale toward R_{gs}, excess energy can be redistributed or radiated into the surrounding interior region $R_{gs} < R \le R_S$. Therefore, the information reservoir is not restricted to the region

$0 \le R \le R_{gs}$ alone. The stable core provides the macroscopic central storage region, while radiation and redistributed degrees of freedom can also occupy the surrounding black hole interior. The essential point is that the information remains within a macroscopic nonsingular interior rather than being compressed into a microscopic remnant.

The same point can be expressed as an order-of-magnitude entropy-capacity estimate. For a physical system of energy $E_{\rm core}$ contained inside a radius $R_{\rm core} \sim R_{gs}$, the Bekenstein bound gives

$$S_{\rm core} \lesssim \frac{2\pi k_B E_{\rm core} R_{\rm core}}{\hbar c}. \tag{224}$$

Writing

$$E_{\rm core} = M_{\rm core} c^2, \qquad R_{\rm core} = \alpha R_S, \qquad \alpha \simeq \frac{5\beta}{7}, \qquad M_{\rm core} = \eta M, \tag{225}$$

where α and η are finite macroscopic fractions, one finds

$$S^{\rm max}_{\rm core} \sim 4\pi\alpha\eta k_B \frac{GM^2}{\hbar c}. \tag{226}$$

This has the same macroscopic mass scaling as the black hole entropy,

$$S_{\rm BH} = \frac{k_B A_S}{4 l_P^2} = 4\pi k_B \frac{GM^2}{\hbar c}, \qquad A_S = 4\pi R_S^2. \tag{227}$$

Thus, the total GSE core is not a fixed microscopic information container. Its possible entropy capacity scales with the size of the original black hole, up to finite factors determined by α and η. This scaling removes the most severe storage difficulty of Planck-scale remnant scenarios [43–48]: the information does not have to be packed into a region whose size is independent of the original black hole mass.

This point is especially natural in the black hole universe interpretation. The information carried by infalling matter is not compressed into a zero volume singularity or into a Planck-scale remnant. It remains associated with an extended macroscopic matter distribution inside the nonsingular core. Since the core radius is a finite fraction of R_S, the interior is a genuine macroscopic physical system, and one may apply the usual expectation that information is preserved in the microscopic state of an extended physical system [7].

This picture also changes the possible late stage of Hawking evaporation. Let

$$R_H(t) = \frac{2GM_{\rm grav}(t)}{c^2} \tag{228}$$

denote the instantaneous Schwarzschild equivalent horizon radius associated with the remaining gravitational mass. In the total GSE dynamics, the collapse does not end in a point singularity, but in a macroscopic nonsingular core with

$$R_{\rm core} \sim R_{gs}. \tag{229}$$

For $\beta \simeq 1$, the total energy at $R = R_{gs}$ gives

$$M_{\rm grav}(R_{gs}) = M_{fr} + \frac{U_{gs-T}(R_{gs})}{c^2} = \frac{13}{20} M_{fr}, \qquad R'_H = \frac{2GM_{\rm grav}(R_{gs})}{c^2} = \frac{13}{20} R_S, \tag{230}$$

whereas

$$R_{gs} = \frac{5}{7} R_S. \tag{231}$$

Thus,

$$R'_H < R_{gs}. \tag{232}$$

In the Schwarzschild equivalent compactness diagnostic, this means that the stabilized core radius exceeds the horizon radius associated with the reduced gravitational mass. If this reduced mass determines the relevant outer horizon after relaxation, the configuration can become horizonless. A complete statement about the global event horizon, however, requires the corresponding time-dependent causal structure.

The conclusion becomes stronger if energy is radiated away during formation or relaxation, or if Hawking evaporation later reduces the exterior gravitational mass. As $M_{\text{grav}}(t)$ decreases, $R_H(t)$ decreases. Once

$$R_H(t) < R_{\text{core}}(t), \tag{233}$$

the object no longer satisfies the horizon-defined black hole condition. The endpoint is then not a Planck-scale remnant or a point singularity, but a horizonless macroscopic nonsingular matter distribution.

For an approximately uniform core, this conclusion is local as well as global. If

$$M(r) = M_{\text{core}} \left(\frac{r}{R_{\text{core}}} \right)^3, \tag{234}$$

then

$$\frac{R_S(r)}{r} = \frac{R_H}{R_{\text{core}}} \left(\frac{r}{R_{\text{core}}} \right)^2. \tag{235}$$

Therefore, when $R_H < R_{\text{core}}$, every inner region also satisfies

$$R_S(r) < r. \tag{236}$$

No inner spherical domain is then locally inside its own Schwarzschild equivalent radius. The interior is converted from a black hole region into a macroscopic nonsingular matter distribution. In this sense, the total GSE dynamics avoids the information storage difficulty of Planck-scale remnants: the information carried by infalling matter remains associated with an extended macroscopic core, and the black hole phase can end when the horizon-defined compactness condition is lost.

Once the horizon-defined compactness condition is lost, the standard steady Hawking evaporation channel need not persist. Nevertheless, transient Hawking-like or dynamical particle creation may continue during the disappearance of the horizon and the subsequent relaxation of the nonsingular core. Determining the late-time radiation flux therefore requires a semiclassical analysis of quantum fields on the time-dependent total GSE geometry.

7 Observational Implications and Tests

7.1 Time-Dependent Dark Energy

The total GSE interpretation of dark energy leads to a time-dependent dark energy density [6]. The dark energy density is not introduced as a strictly constant vacuum term. It is determined by the matter density inside the causal domain, the causal radius, and the structure coefficient, with the Schwarzschild equivalent radius following from the enclosed matter-sector mass through $R_S(t) = 2GM(t)/c^2$. We write

$$\rho_{\Lambda_m}(t) = \frac{\beta(t)\rho_m(t)}{2} \frac{R_S(t)}{R_U(t)} \left[\frac{5\beta(t)}{14} \frac{R_S(t)}{R_U(t)} - 1 \right]. \tag{237}$$

Here $R_U(t)$, $M(t)$, and $\beta(t)$ retain the meanings defined above: the observer-centered causal radius, the enclosed matter-sector mass, and the structural coefficient of the matter distribution, respectively. Here $\beta(t)$ denotes the structural integration coefficient of the GSE functional. For a uniform spherical distribution in the Newtonian limit, $\beta = 3/5$. For relativistic or compact self-gravitating configurations, β is naturally of order unity, typically $\beta \sim$ 1–2. After large-scale structure formation, the large-scale matter distribution evolves slowly, and therefore $\beta(t)$ may be approximated by a constant value except in the very early universe.

Equation (237) gives a direct observational target. If the total GSE interpretation is correct, the inferred dark energy density should not behave as a completely independent constant. It should be related to the matter content inside the causal horizon, the growth of the causal horizon scale, and the evolution of the ratio $\frac{R_S(t)}{R_U(t)}$. Thus, measurements of the expansion history, the effective equation-of-state parameter $w(z)$, and the possible redshift evolution of dark energy provide direct tests of the model.

The sign of the dark energy sector follows from the factor

$$\left[\frac{5\beta(t)}{14}\frac{R_S(t)}{R_U(t)} - 1\right]. \tag{238}$$

The sign transition occurs when

$$R_U(t) = \frac{5\beta(t)}{14} R_S(t). \tag{239}$$

The total GSE dark energy density is positive when $R_U(t) < \frac{5\beta(t)}{14} R_S(t)$, and negative when $R_U(t) > \frac{5\beta(t)}{14} R_S(t)$.

However, a positive value of ρ_{Λ_m} is not sufficient by itself to produce accelerated expansion. In a matter-dominated epoch, following the standard ΛCDM background description in which dark energy is represented by a cosmological-constant-like component with $w_\Lambda = -1$ [15,23], we adopt the corresponding approximation $w_{\Lambda_m} \simeq -1$ for the positive total GSE dark energy sector. The approximation $w_{\Lambda_m} \simeq -1$ applies when the total GSE dark energy density varies slowly over a Hubble time.

Under this approximation, the acceleration condition is

$$\rho_{\Lambda_m}(t) > \frac{1}{2}\rho_m(t). \tag{240}$$

Equivalently, the causal domain enters the accelerated-expansion regime when

$$R_U(t) < R_{\mathrm{crit,U}}(t), \tag{241}$$

where

$$R_{\mathrm{crit,U}}(t) \simeq 0.279\,\beta(t) R_S(t). \tag{242}$$

Therefore, the model predicts two distinct observational transitions. The first is the sign transition of the total GSE dark energy density, where ρ_{Λ_m} changes sign. The second is the acceleration transition, where ρ_{Λ_m} becomes larger than $\rho_m/2$. These two transitions need not occur at the same redshift. Observational reconstruction of $H(z)$, $q(z)$, and $w(z)$ can therefore be used to test whether the dark energy sector follows the time-dependent total GSE form in Eq. (237).

Recent observational programs that constrain the redshift evolution of the dark energy sector provide a direct arena for testing this time-dependent prediction [16].

7.2 Cosmic Expansion History

The total GSE dynamics gives a unified qualitative sequence for the expansion history of the universe [6]:

$$
\begin{aligned}
&\text{early acceleration driven by total GSE (inflation)} \\
&\longrightarrow \text{a decelerating phase during the radiation era and the matter era} \\
&\longrightarrow \text{late-time total GSE dark energy acceleration.}
\end{aligned}
\tag{243}
$$

Accelerated expansion arises when the total GSE contribution of the causal domain becomes a sufficiently large positive dark energy density.

The expansion history can be organized into three linked stages.

1) **Early total GSE accelerated expansion.**

   The first stage corresponds to the very early high-density and high-compactness regime. In this phase, the total GSE dark energy density can exceed the radiation density:

   $$\rho_{\Lambda_m} > \rho_r. \tag{244}$$

   With an effective equation of state $w_{\Lambda_m} \simeq -1$, this produces negative pressure and drives an inflation-like accelerated expansion. The order-of-magnitude trigger estimate discussed in Sec. 5.3 shows that the total GSE mechanism can reach the characteristic time and energy density scales usually associated with the standard inflationary epoch [6].

2) **Radiation- and matter-dominated decelerating expansion.**

   The second stage begins when the early total GSE dark energy contribution weakens as the causal scale expands. Once

   $$\rho_{\Lambda_m} < \rho_r, \tag{245}$$

   the radiation component dominates the acceleration equation and the universe enters a decelerating radiation era. After the radiation-to-matter transition, the matter-dominated era remains decelerating as long as

   $$\rho_{\Lambda_m} < \frac{1}{2}\rho_m. \tag{246}$$

   This middle epoch is not merely a passive decelerating period. In the regime

   $$\rho_{\Lambda_m} < 0, \tag{247}$$

   the total GSE contribution enters the effective acceleration equation in the attractive direction. Therefore, it can enhance gravitational clustering rather than suppress it. In this sense, the negative total GSE phase naturally supports the formation of large-scale structure.

   This feature is important for the interpretation of early structure formation. If the total GSE contribution is negative during part of the radiation- and matter-dominated eras, it provides an additional attractive background contribution that can make the growth of density perturbations more efficient than in a model with only a positive repulsive dark energy sector. At the background level, the same total GSE density function that later produces cosmic acceleration can therefore provide a possible route to enhanced early structure growth, including the early assembly of candidate massive galaxies reported by JWST [6, 40, 41]. A full quantitative treatment requires a perturbation-level analysis of structure growth, but at the background level the sign of ρ_{Λ_m} already shows why this era can favor structure formation.

3) **Late-time total GSE dark energy acceleration.**

The third stage occurs at late times. As the physical particle horizon, or more generally the observer-centered causal horizon, expands, new matter and galaxies enter the causally connected domain. The enclosed matter-sector mass $M(t)$ increases, and the associated Schwarzschild equivalent radius $R_S(t) = \frac{2GM(t)}{c^2}$ grows relative to $R_U(t)$. In a simple uniform spherical estimate,

$$M(t) \propto R_U(t)^3, \qquad R_S(t) \propto R_U(t)^3, \qquad \frac{R_S(t)}{R_U(t)} \propto R_U(t)^2. \tag{248}$$

This growth drives the total GSE dark energy density from negative to positive, and eventually into the acceleration regime

$$\rho_{\Lambda_m} > \frac{1}{2}\rho_m. \tag{249}$$

The expansion history therefore provides a multi-epoch test. A successful version of the model must reproduce three linked features using the same total GSE density function:

- an early accelerated phase when $\rho_{\Lambda_m} \gtrsim \rho_r$;
- an intermediate decelerating era when ρ_{Λ_m} is negative or too small to dominate radiation and matter, with the negative phase supporting gravitational structure formation;
- a late-time acceleration transition when $\rho_{\Lambda_m} > \rho_m/2$.

This structure differs from a model in which primordial inflation and late-time dark energy are introduced as two unrelated sectors. In the present framework, both accelerated epochs arise from the same total GSE dark energy density, while the intermediate decelerating era appears when this contribution becomes subdominant or negative. The negative phase is also physically useful: it enhances gravitational clustering and helps account for the early appearance of massive galaxies and massive black holes [6, 40, 41].

7.3 Black Hole Interior Predictions

The total GSE dynamics that gives the dark energy density also predicts a modified interior structure for black holes [7]. In this framework, a black hole interior is not driven toward an unbounded point singularity. Instead, the total GSE energy landscape contains finite characteristic radii. The stable equilibrium radius is

$$R_{gs} = \frac{5\beta}{7} R_S, \tag{250}$$

and the energy-limited radii include

$$R_{\min,E} = \frac{5\beta}{14} R_S, \qquad R_{\min,BH} = \frac{5\beta}{14 - 5\beta} R_S. \tag{251}$$

Here $R_{\min,BH}$ is meaningful in this form for $14 - 5\beta > 0$. For $0 < \beta < 7/5$, R_{gs} lies inside R_S. For representative values of β of order unity, and in particular for the fiducial interior value $\beta \simeq 1$, these radii are macroscopic for stellar-mass and supermassive black holes [7].

The total GSE structure also modifies the mass-energy bookkeeping of a compact object [7]. If the GSE is ignored, the exterior gravitational field is associated only with the free-state matter mass. If only the single attractive GSE term is included, the bound configuration receives a negative binding energy correction. In the total GSE framework, however, the additional positive matter–GSE interaction term is also present:

$$U_{gs-T}(R) = -\beta \frac{GM_{fr}^2}{R}\left(1 - \frac{5\beta}{7}\frac{GM_{fr}}{c^2R}\right). \tag{252}$$

Thus, the effective gravitational mass-energy of the bound object is shifted not only by the attractive GSE term, but also by the positive energy contribution responsible for the repulsive radial response. Schematically, the equivalent mass can be represented by the total bound energy,

$$M_{\text{grav}} \sim M_{fr} + \frac{U_{gs-T}}{c^2}, \tag{253}$$

rather than by the free-state matter mass alone [7].

This gives several compact object implications. First, the model predicts nonsingular finite-radius cores rather than point singularities. Second, the internal mass distribution can undergo stabilization, virialization, and energy redistribution before reaching the classical singular limit. Third, the exterior spacetime can remain close to the standard black hole geometry while the deep interior and the effective mass-energy bookkeeping are modified by the total GSE structure [7].

Direct observation of the black hole interior is difficult. However, the present framework provides an additional observational route. Using the matter density ρ_m, the compactness of the present observable universe is

$$\frac{R_S}{R_U} \simeq 3.23, \tag{254}$$

while using the critical density ρ_c as a comparison scale gives

$$\frac{R_{S,c}}{R_U} \simeq 10.3. \tag{255}$$

In both cases, the observable universe radius R_U lies well inside the corresponding Schwarzschild-equivalent radius scale. Thus, in the Schwarzschild equivalent compactness sense, the observable universe exists inside a cosmological black hole domain generated by its own enclosed equivalent mass. Cosmological observations can therefore probe the same total GSE structure that governs black hole interiors [6, 7].

In particular, the sign transition of the total GSE dark energy density occurs when

$$\rho_{\Lambda_m} = 0 \quad \Longleftrightarrow \quad R_U = \frac{5\beta}{14}R_S = R_{\min,E}. \tag{256}$$

Therefore, the epoch at which the inferred dark energy density changes sign provides an indirect test of the total GSE structure near $R_{\min,E}$. In an ordinary black hole, $R_{\min,E}$ appears as the zero of the total GSE energy and as an energy-limited characteristic radius. In cosmology, the same algebraic radius appears as the compactness threshold at which the total GSE dark energy density changes sign.

This connection is important for Black Hole Cosmology. Since the observable universe satisfies $R_U < R_S$ in the Schwarzschild equivalent compactness sense, the cosmic history of $\rho_{\Lambda_m}(t)$ can be interpreted as an indirect observational window into the total GSE interior dynamics of a cosmological black hole. The transition from negative ρ_{Λ_m}, to positive ρ_{Λ_m}, and finally to $\rho_{\Lambda_m} > \rho_m/2$ is not only a cosmological prediction [6]. It is also an indirect test of the finite-radius total GSE structure that replaces the black hole singularity.

The model therefore motivates two complementary classes of tests.

The first class is astrophysical: searches for indirect signatures of nonsingular interiors, such as deviations in late-stage collapse, possible modifications of compact object ringdown spectra, changes in the effective compactness of ultracompact objects, or phenomenological constraints from black hole formation and accretion [7,49–51]. Outside the stable radius R_{gs}, and in particular even near the Schwarzschild equivalent horizon scale, the positive matter–GSE interaction term partially cancels the radial derivative of the attractive GSE term. The total radial response remains attractive for $R > R_{gs}$, but its magnitude is reduced relative to the single attractive GSE contribution. Thus, in the total GSE dynamics, the inward contraction of a highly compact object is weakened before the system reaches the finite-radius stabilization regime.

The second class is cosmological: reconstruction of $\rho_{\Lambda_m}(t)$, the sign transition epoch, the acceleration transition epoch, and the relation between $R_U(t)$, $R_S(t)$, and $R_{\min,E}(t)$. These signatures require detailed modeling, but the qualitative prediction is specific: the physical endpoint of collapse is a finite-radius core, and the same total GSE radius structure appears observationally in the dark energy history of our cosmological black hole [6].

8 Conclusion

Black Hole Cosmology has historically faced three major objections. A classical black hole interior appears to terminate at a future singularity, whereas standard cosmology places the Big-Bang singularity in the past. The conventional black hole interior picture also seems to leave no large stable region in which galaxies, stars, planets, and observers can exist. Finally, the observed expansion and late-time accelerated expansion of the universe have usually been regarded as evidence against the idea that the universe is related to a black hole configuration [5].

In this paper, we use total gravitational self-energy (GSE) to reassess these objections. We argue that some of the objections rest on an internally incomplete premise, namely the classical black hole interior picture that itself terminates in a singularity, while the remaining problems can be addressed within the Black Hole Cosmology framework once total GSE dynamics is included.

The central physical input is

$$U_{gs-T}(R) = -\beta \frac{GM_{fr}^2}{R}\left(1 - \frac{5\beta}{7}\frac{GM_{fr}}{c^2 R}\right). \tag{257}$$

The first term is the negative GSE term, while the second term is the positive matter–GSE interaction-energy contribution [6, 7]. For a matter-filled black hole interior, the radial response follows from

$$D_T U = -\frac{1}{M_{fr}}\frac{dU_{gs-T}}{dR}. \tag{258}$$

This dynamics contains the stable GSE radius and the energy-limited radii

$$R_{gs} = \frac{5\beta}{7}R_S, \qquad R_{\min,E} = \frac{5\beta}{14}R_S, \qquad R_{\min,BH} = \frac{5\beta}{14-5\beta}R_S. \tag{259}$$

In the present framework, these finite radii replace the point singularity with a finite-radius structure [7]. For sufficiently massive black holes, the characteristic radii are macroscopic, allowing the possibility of a closed black hole universe with a broad nonsingular interior region. In principle, such an interior can be large enough to contain galaxies, stars, planets, and intelligent observers [5,7].

Our observable universe is more naturally described by a second interpretation. The present framework does not require the entire universe to be an isolated Schwarzschild black hole surrounded by an exterior vacuum. Matter and energy may be distributed nearly uniformly over a region much larger than the present observable universe. In this case, the relevant object is the observer-centered causal patch. The matter-sector mass contained inside the physical particle horizon, or more generally inside the observer-centered causal horizon, defines the Schwarzschild-equivalent event horizon radius

$$R_S(t) = \frac{2GM(t)}{c^2}. \tag{260}$$

For the present observable universe,

$$R_S \simeq 150.4\,\text{Gly}, \qquad R_U \simeq 46.5\,\text{Gly}, \tag{261}$$

and therefore

$$\frac{R_S}{R_U} \simeq 3.23 > 1. \tag{262}$$

Thus, in the Schwarzschild equivalent compactness sense, the observable universe lies inside the event horizon scale generated by its own enclosed matter-sector mass. This does not mean that the whole universe is a finite isolated vacuum black hole. It means that our observable universe is a high-compactness cosmological black hole domain embedded inside a much larger nearly homogeneous cosmic matter distribution.

This compactness result sharpens the limitation of classical general relativity. Classical general relativity predicts a singularity at the endpoint of black hole collapse, indicating that the unmodified classical theory is not a complete description of black hole interiors. Therefore,

> **If General Relativity is incomplete inside a black hole, then it is also incomplete in the observable universe. Its incompleteness therefore necessitates additional ingredients such as inflaton field and dark energy.**

The reason is that the observable universe itself satisfies a compactness condition of a black hole interior. In this framework, dark energy is not an independent component added by hand to cosmology. It is interpreted as the cosmological manifestation of the total GSE contribution that becomes important in a black hole interior compactness regime [6,7].

In cosmology, $R_U(t)$ is the causal radius of the observable domain, not the surface of a finite isolated object. The total GSE of the matter-sector mass inside this causal domain appears as a total GSE dark energy density,

$$\rho_{\Lambda_m} = \frac{\beta\rho_m}{2}\frac{R_S}{R_U}\left(\frac{5\beta}{14}\frac{R_S}{R_U} - 1\right). \tag{263}$$

The sign transition occurs at

$$R_U = \frac{5\beta}{14}R_S = R_{\min,E}. \tag{264}$$

For $R_U < R_{\min,E}$, the total GSE dark energy density becomes positive. When the fractional variation of ρ_{Λ_m} is small on the Hubble timescale, its effective equation-of-state parameter approaches $w_{\Lambda_m} \simeq -1$. The corresponding negative pressure can then drive accelerated expansion once ρ_{Λ_m} becomes sufficiently large. In a matter-dominated epoch, the acceleration condition is

$$\rho_{\Lambda_m} > \frac{1}{2}\rho_m, \tag{265}$$

or equivalently

$$R_U < R_{\mathrm{crit,U}}, \qquad R_{\mathrm{crit,U}} \simeq 0.279\,\beta R_S. \tag{266}$$

For the present observable universe, using

$$\rho_{m,0} = 0.315\rho_c, \qquad R_U \simeq 46.5\,\mathrm{Gly}, \qquad R_S \simeq 150.4\,\mathrm{Gly}, \qquad \beta = 1.595, \tag{267}$$

the model gives

$$\rho_{\Lambda_m} \simeq 0.685\rho_c. \tag{268}$$

This value is consistent with the observed magnitude of the present dark energy density [6,15].

The total GSE dynamics gives a three-stage interpretation of cosmic history:

$$\begin{aligned} &\text{early acceleration driven by total GSE (inflation)} \\ \longrightarrow\ &\text{a decelerating phase during the radiation era and the matter era} \\ \longrightarrow\ &\text{late-time total GSE dark energy acceleration.} \end{aligned} \tag{269}$$

In the very early universe, the causal domain is extremely compact, and ρ_{Λ_m} can exceed the radiation density, producing an inflation-like accelerated phase. As the causal domain expands, the compactness factor weakens and the universe enters radiation- and matter-dominated deceleration. At late times, as the causal horizon grows, newly connected matter enters the causal domain, and the Schwarzschild-equivalent radius grows relative to R_U. This makes ρ_{Λ_m} positive and eventually large enough to satisfy the acceleration condition [6].

The framework also gives observational and astrophysical tests. Cosmologically, the model predicts a sign transition of ρ_{Λ_m}, an acceleration transition when $\rho_{\Lambda_m} > \rho_m/2$, and a possible mild time dependence of dark energy near the present epoch [6]. Astrophysically, it predicts that black hole collapse ends in a finite-radius structure characterized by R_{gs}, $R_{\min,E}$, and $R_{\min,BH}$, rather than in a point singularity. Since the observable universe satisfies $R_U < R_S$ in the Schwarzschild equivalent compactness sense, the cosmic sign transition near $R_U = R_{\min,E}$ also provides an indirect observational window into the same total GSE structure that replaces the black hole singularity.

The central conclusion is therefore a reversal of the historical objection to Black Hole Cosmology. Cosmic expansion is not evidence against Black Hole Cosmology. In the present framework, accelerated expansion is one of its main physical signatures. From the inflationary epoch to the present, the observable universe has remained inside the Schwarzschild equivalent cosmological black hole domain generated by its own enclosed matter-sector mass. Its cosmic history is therefore described as having unfolded inside a cosmological black hole domain, and the observed dark energy is the signature of the total GSE structure operating within that domain [6,7].

Acknowledgements. All original scientific ideas, physical interpretations, and theoretical proposals presented in this work are the author's own. In particular, the reformulation of Black Hole Cosmology using total GSE, the distinction between a closed black hole universe and a cosmological black hole causal domain, the finite-radius interpretation of black hole interiors and the interpretation of the observable universe as a high-compactness causal domain inside its own Schwarzschild-equivalent radius were conceived by the author. The total GSE dark energy density function, its sign transition near $R_U = R_{\min,E}$, the acceleration threshold $R_{\mathrm{crit,U}}$, and the interpretation of cosmic accelerated expansion as evidence for the Black Hole Cosmology are also original contributions of the author. The present work further develops ideas from the author's earlier studies on total GSE, Matter-Only Cosmology (MOC), and

black hole interiors, and synthesizes them into a revised formulation of Black Hole Cosmology. Generative AI was used during the drafting and editing process to assist with exposition, and language refinement. The final manuscript was independently reviewed and verified by the author, who assumes full responsibility for all scientific claims, calculations, interpretations, and conclusions.

A Derivation of the Total GSE Functional

This appendix summarizes the derivation of the total gravitational self-energy (GSE) functional used in the main text. The purpose is to show how the ordinary attractive GSE term is completed by a positive matter–GSE interaction term once the equivalent mass associated with GSE is included in the gravitational source bookkeeping. This derivation was presented in the preceding Matter-Only Cosmology (MOC) framework [6] and is reproduced here in a condensed form for its application to Black Hole Cosmology.

A.1 Equivalent Gravitational Source

For a self-gravitating spherical matter distribution, the conventional differential GSE contribution is written as

$$dU_{gs} = -G\frac{M'(r)}{r}\,dM, \tag{270}$$

where $M'(r)$ is the matter mass enclosed inside radius r, and dM is the mass of the infinitesimal spherical shell. In the standard Newtonian calculation, $M'(r)$ is taken to be the free matter source.

In general relativity, however, all forms of energy contribute to the gravitational source [8, 17]. In the present framework, the gravitational self-energy of the interior region is therefore included as part of the equivalent source of the self-gravitating system. This is a system-level mass-energy bookkeeping prescription; it is not a local stress-energy tensor of the gravitational field itself.

The GSE of the interior sphere is parameterized as

$$U_{gs}(r) = -\beta\frac{GM'(r)^2}{r}, \tag{271}$$

where β is the structural coefficient of the GSE functional. For a uniform Newtonian sphere, $\beta = 3/5$, while more compact or centrally concentrated self-gravitating configurations generally correspond to coefficients of order unity [31, 32, 34].

The signed equivalent mass associated with the interior GSE is

$$\frac{U_{gs}(r)}{c^2} = -\beta\frac{GM'(r)^2}{rc^2}. \tag{272}$$

Equivalently, defining the positive magnitude

$$M'_{gs}(r) \equiv \frac{|U_{gs}(r)|}{c^2} = \beta\frac{GM'(r)^2}{rc^2}, \tag{273}$$

the equivalent source becomes

$$M_{\text{eq}}(r) = M'(r) - M'_{gs}(r). \tag{274}$$

Thus,

$$M_{\text{eq}}(r) = M'(r)\left(1-\beta\frac{GM'(r)}{rc^2}\right). \tag{275}$$

A.2 Uniform Density Derivation

The total GSE is obtained by inserting the equivalent source $M_{\text{eq}}(r)$ into the binding energy integral:

$$U_{gs-T} = \int_0^R dU_{gs-T} = \int_0^R -G\frac{M_{\text{eq}}(r)}{r}\,dM. \tag{276}$$

For analytical clarity, take a uniform density ρ. Then

$$M'(r) = \frac{4\pi}{3}\rho r^3, \qquad dM = 4\pi r^2 \rho\, dr. \tag{277}$$

Substituting Eqs. (275) and (277) into Eq. (276) gives

$$\begin{aligned} U_{gs-T} &= -4\pi G\rho \int_0^R r\left[M'(r) - \frac{\beta G}{c^2}\frac{M'(r)^2}{r}\right]dr \\ &= \int_0^R \left[-\frac{16\pi^2 G\rho^2}{3}r^4 + \frac{64\pi^3\beta G^2\rho^3}{9c^2}r^6\right]dr. \end{aligned} \tag{278}$$

Performing the integration yields

$$U_{\text{gs-T}} = \frac{3}{5}\left[-\frac{16\pi^2 G\rho^2 R^5}{9} + \frac{320\pi^3\beta G^2\rho^3 R^7}{189c^2}\right]. \tag{279}$$

To account for the relativistic contributions and the geometric distribution of mass in a general self-gravitating system, we generalize the Newtonian coefficient $3/5$ to the structure coefficient β. This replacement follows from consistently applying the original structural generalization ($3/5 \to \beta$) to the integrated self-energy expression. Since the first term of $U_{\text{gs-T}}$ is precisely the matter GSE defined in Eq. (271), it must carry the same coefficient β.

$$U_{\text{gs-T}} = \beta\left[-\frac{16\pi^2 G\rho^2 R^5}{9} + \frac{320\pi^3\beta G^2\rho^3 R^7}{189c^2}\right]. \tag{280}$$

$$U_{gs-T}(R) = -\beta\frac{GM_{fr}^2}{R} + \frac{5}{7}\beta^2\frac{G^2 M_{fr}^3}{c^2R^2}. \tag{281}$$

Equivalently,

$$U_{gs-T}(R) = -\beta\frac{GM_{fr}^2}{R}\left(1 - \frac{5\beta}{7}\frac{GM_{fr}}{c^2R}\right). \tag{282}$$

Equation (281) shows the origin of the two-term structure. The first term is the ordinary negative GSE contribution. The second term is positive and arises from the interaction between matter and the equivalent mass associated with its own GSE.

A.3 Density Decomposition

Dividing the total GSE by c^2V, where $V = \frac{4\pi}{3}R^3$, $\rho_m = \frac{M_{fr}}{V}$, gives the total GSE density. The negative attractive component is

$$-\rho_{gs} = -\frac{1}{Vc^2}\beta\frac{GM_{fr}^2}{R} = -\frac{4\pi\beta G}{3c^2}\rho_m^2R^2. \tag{283}$$

Here $\rho_{gs} > 0$ denotes the positive magnitude of the attractive GSE density, while the actual equivalent density contribution is $-\rho_{gs}$.

The positive matter–GSE interaction density is

$$\rho_{m-gs} = \frac{1}{Vc^2}\frac{5}{7}\beta^2\frac{G^2M_{fr}^3}{c^2R^2} = \frac{80\pi^2\beta^2G^2}{63c^4}\rho_m^3R^4. \tag{284}$$

The net total GSE density is therefore

$$\rho_{\Lambda_m} \equiv (\rho_{m-gs}) + (-\rho_{gs}) = \rho_{m-gs} - \rho_{gs}. \tag{285}$$

Using Eqs. (283) and (284), this becomes

$$\rho_{\Lambda_m}(\rho_m, R) = \frac{4\pi\beta G}{3c^2}\rho_m^2R^2\left[\left(\frac{20\pi\beta G}{21c^2}\right)\rho_mR^2 - 1\right]. \tag{286}$$

Defining

$$k_1 \equiv \frac{4\pi G}{3c^2}, \qquad k_2 \equiv \frac{20\pi G}{21c^2}, \tag{287}$$

one may write

$$\rho_{\Lambda_m}(\rho_m, R) = k_1\beta\rho_m^2R^2\left(k_2\beta\rho_mR^2 - 1\right). \tag{288}$$

Finally, using

$$R_S = \frac{2GM_{fr}}{c^2}, \qquad \frac{R_S}{R} = \frac{8\pi G}{3c^2}\rho_mR^2, \tag{289}$$

the same density can be expressed in the compactness form

$$\rho_{\Lambda_m} = \frac{\beta\rho_m}{2}\frac{R_S}{R}\left(\frac{5\beta}{14}\frac{R_S}{R} - 1\right). \tag{290}$$

In the cosmological application, R is replaced by the causal radius $R_U(t)$, and M_{fr} is replaced by the enclosed matter sector mass $M(t)$. Thus, Eq. (290) becomes the total GSE dark energy density used in the cosmological sections of the paper.

References

[1] Pathria, R. K. The Universe as a Black Hole. *Nature*, **240**, 298–299 (1972).

[2] Good, I. J. Chinese universes. *Physics Today*, **25**(7), 15 (1972).

[3] Frolov, V. P., Markov, M. A., & Mukhanov, V. F. Black holes as possible sources of closed and semiclosed worlds. *Phys. Rev. D*, **41**(2), 383–394 (1990).

[4] Frolov, V. P., Markov, M. A., & Mukhanov, V. F. Through a black hole into a new universe? *Phys. Lett. B*, **216**(3-4), 272–276 (1989).

[5] Choi, H. *Problems and Solutions of Black Hole Cosmology*. Preprint (2022). Available at: https://www.researchgate.net/publication/359192496.

[6] Choi, H. *Matter-Only Cosmology: A Unified Origin for Inflation and Dark Energy*. Preprint (2025). Available at: https://www.researchgate.net/publication/398004497.

[7] Choi, H. *The Physical Origin of the Planck Scale Cutoff and Completion of Perturbative Quantum Gravity*. Preprint (2025). Available at: https://www.researchgate.net/publication/397952460.

[8] Misner, C. W., Thorne, K. S., & Wheeler, J. A. *Gravitation*. (W. H. Freeman, San Francisco, 1973).

[9] Oppenheimer, J. R., & Snyder, H. On Continued Gravitational Contraction. *Phys. Rev.*, **56**(5), 455–459 (1939).

[10] Shapiro, S. L., & Teukolsky, S. A. *Black Holes, White Dwarfs, and Neutron Stars: The Physics of Compact Objects*. (John Wiley & Sons, New York, 1983).

[11] Penrose, R. Gravitational Collapse and Space-Time Singularities. *Phys. Rev. Lett.*, **14**(3), 57–59 (1965).

[12] Weinberg, S. *Gravitation and Cosmology: Principles and Applications of the General Theory of Relativity*. (John Wiley & Sons, New York, 1972).

[13] Riess, A. G., et al. Observational Evidence from Supernovae for an Accelerating Universe and a Cosmological Constant. *Astron. J.*, **116**(3), 1009–1038 (1998).

[14] Perlmutter, S., et al. Measurements of Ω and Λ from 42 High-Redshift Supernovae. *Astrophys. J.*, **517**(2), 565–586 (1999).

[15] Planck Collaboration. Planck 2018 results. VI. Cosmological parameters. *Astron. Astrophys.*, **641**, A6 (2020). arXiv:1807.06209 [astro-ph.CO].

[16] Adame, A. G., et al. [DESI Collaboration]. DESI 2024 VI: Cosmological Constraints from the Measurements of Baryon Acoustic Oscillations. (2024). arXiv:2404.03002 [astro-ph.CO].

[17] Wald, R. M. *General Relativity*. (University of Chicago Press, Chicago, 1984).

[18] Guth, A. H. Inflationary Universe: A Possible Solution to the Horizon and Flatness Problems. *Phys. Rev. D*, **23**(2), 347–356 (1981).

[19] Albrecht, A., & Steinhardt, P. J. Cosmology for Grand Unified Theories with Radiatively Induced Symmetry Breaking. *Phys. Rev. Lett.*, **48**(17), 1220–1223 (1982).

[20] Linde, A. D. A New Inflationary Universe Scenario: A Possible Solution of the Horizon, Flatness, Homogeneity, Isotropy and Primordial Monopole Problems. *Phys. Lett. B*, **108**(6), 389–393 (1982).

[21] Binney, J., & Tremaine, S. *Galactic Dynamics*, 2nd ed. (Princeton University Press, Princeton, NJ, 2008).

[22] Navarro, J. F., Frenk, C. S., & White, S. D. M. A Universal Density Profile from Hierarchical Clustering. *Astrophys. J.*, **490**(2), 493–508 (1997).

[23] Carroll, S. M. The Cosmological Constant. *Living Rev. Relativ.*, **4**, 1 (2001).

[24] Ashtekar, A., Olmedo, J., & Singh, P. Quantum Transfiguration of Kruskal Black Holes. *Phys. Rev. Lett.*, **121**(24), 241301 (2018).

[25] Rovelli, C., & Vidotto, F. Planck stars. *Int. J. Mod. Phys. D*, **23**(12), 1442026 (2014). arXiv:1401.6562 [gr-qc].

[26] 't Hooft, G., & Veltman, M. One-loop divergencies in the theory of gravitation. *Annales de l'Institut Henri Poincaré Section A: Physique théorique*, **20**(1), 69–94 (1974).

[27] Burgess, C. P. Quantum gravity in everyday life: General relativity as an effective field theory. *Living Rev. Relativ.*, **7**(1), 5 (2004).

[28] Goroff, M. H., & Sagnotti, A. Quantum gravity at two loops. *Phys. Lett. B*, **160**(1), 81–86 (1985).

[29] Weinberg, S. Ultraviolet divergences in quantum theories of gravitation. In *General Relativity: An Einstein Centenary Survey*, edited by S. W. Hawking and W. Israel (Cambridge University Press, Cambridge, 1979), pp. 790–831.

[30] Polchinski, J. *String Theory*, Vols. 1–2. (Cambridge University Press, Cambridge, 1998).

[31] Thornton, S. T., & Marion, J. B. *Classical Dynamics of Particles and Systems*, 5th ed. (Brooks/Cole, Belmont, CA, 2004).

[32] E. Alécian and S. M. Morsink, "The Effect of Neutron Star Gravitational-Binding Energy on Gravitational-Radiation-Driven Mass-Transfer Binaries," Astrophys. J. **614**, 914–921 (2004), arXiv:astro-ph/0302219.

[33] A. A. Dutton and A. V. Macciò, "Cold dark matter haloes in the Planck era: evolution of structural parameters for Einasto and NFW profiles," Mon. Not. R. Astron. Soc. **441**, 3359–3374 (2014).

[34] Chandrasekhar, S. *An Introduction to the Study of Stellar Structure*. (University of Chicago Press, Chicago, 1939).

[35] Carroll, B. W., & Ostlie, D. A. *An Introduction to Modern Astrophysics*, 2nd ed. (Pearson Addison-Wesley, San Francisco, 2007).

[36] Arnowitt, R., Deser, S., & Misner, C. W. The Dynamics of General Relativity. In *Gravitation: An Introduction to Current Research*, edited by L. Witten (Wiley, New York, 1962), pp. 227–265. Reprinted as arXiv:gr-qc/0405109.

[37] Misner, C. W., & Sharp, D. H. Relativistic Equations for Adiabatic, Spherically Symmetric Gravitational Collapse. *Physical Review* **136**, B571–B576 (1964). doi:10.1103/PhysRev.136.B571.

[38] Choi, H. *Dark Energy is Gravitational Potential Energy or Energy of the Gravitational Field*. Preprint (2022). Available at: https://www.researchgate.net/publication/360096238.

[39] Starobinsky, A. A. A New Type of Isotropic Cosmological Models Without Singularity. *Phys. Lett. B*, **91**(1), 99–102 (1980).

[40] I. Labbé *et al.*, "A population of red candidate massive galaxies at $z > 10$," Nature **616**, 266–269 (2023).

[41] M. Boylan-Kolchin, "Stress testing ΛCDM with high-redshift galaxy candidates," Nat. Astron. **7**, 731–735 (2023).

[42] P. A. Burger *et al.* (KiDS-1000 Collaboration), "KiDS-1000 cosmology: Constraints from density split statistics," Astron. Astrophys. **669**, A69 (2023).

[43] Hawking, S. W. Breakdown of Predictability in Gravitational Collapse. *Phys. Rev. D*, **14**(10), 2460–2473 (1976).

[44] Hawking, S. W. Particle Creation by Black Holes. *Commun. Math. Phys.*, **43**(3), 199–220 (1975).

[45] Page, D. N. Information in Black Hole Radiation. *Phys. Rev. Lett.*, **71**(23), 3743–3746 (1993).

[46] Harlow, D. Jerusalem Lectures on Black Holes and Quantum Information. *Rev. Mod. Phys.*, **88**(1), 015002 (2016).

[47] Bekenstein, J. D. Black Holes and Entropy. *Phys. Rev. D*, **7**(8), 2333–2346 (1973).

[48] Bekenstein, J. D. Universal Upper Bound on the Entropy-to-Energy Ratio for Bounded Systems. *Phys. Rev. D*, **23**(2), 287–298 (1981).

[49] Berti, E., Cardoso, V., & Starinets, A. O. Quasinormal modes of black holes and black branes. *Class. Quantum Grav.*, **26**(16), 163001 (2009).

[50] Abbott, B. P. et al. (LIGO Scientific Collaboration and Virgo Collaboration). Observation of Gravitational Waves from a Binary Black Hole Merger. *Phys. Rev. Lett.*, **116**(6), 061102 (2016).

[51] Bambi, C. Testing black hole candidates with electromagnetic radiation. *Rev. Mod. Phys.*, **89**(2), 025001 (2017).